2015

# Analysis of ground vibrations produced by an 80 in3 water gun in the Chicago Sanitary and Ship Canal, Lemont, Illinois

Carolyn Michelle Koebel

ABSTRACT

ANALYSIS OF GROUND VIBRATIONS PRODUCED
BY AN 80 IN$^3$ WATER GUN IN THE CHICAGO
SANITARY AND SHIP CANAL,
LEMONT, ILLINOIS

Carolyn M. Koebel, M.S.
Department of Geology and Environmental Geosciences
Northern Illinois University, 2015
Philip J. Carpenter, Director

Since its completion in 1910, the Chicago Sanitary and Ship Canal (CSSC) has become a pathway for invasive species (and potentially Asian carp) to reach the Great Lakes. Currently, an electric barrier is used to prevent Asian carp migration through the canal, but the need for a secondary method is necessary, especially when the electric barrier undergoes maintenance. The underwater Asian carp "cannon" (water gun) provides such a method. Analysis of the ground movement produced by an 80 in$^3$ water gun in the CSSC was performed in order to establish any potential for damage to the either the canal or structures built along the canal. Ground movement was collected using 3-component geophones on both the land surface and in boreholes. The peak particle velocities (PPVs) were analyzed to determine if damage would be caused to structures located along the canal. Vector sum velocity ground movement along the canal wall was as high as 0.28 in/s (7.11 mm/s), which is much lower than the United States Bureau of Mines (USBM) ground vibration damage threshold of 0.75 in/s (19.1 mm/s), causing no potential for damage to structures along the canal wall. The dominant frequency of ground motion produced by the water gun is primarily above 40 Hz, so the wave energy should attenuate fairly quickly away from the canal wall, with little disturbance to structures further from the wall.

NORTHERN ILLINOIS UNIVERSITY
DEKALB, ILLINOIS

AUGUST 2015

# ANALYSIS OF GROUND VIBRATIONS PRODUCED BY AN 80 $IN^3$ WATER GUN IN THE CHICAGO SANITARY AND SHIP CANAL, LEMONT, ILLINOIS

BY

CAROLYN MICHELLE KOEBEL

A THESIS SUBMITTED TO THE GRADUATE SCHOOL

IN PARTIAL FULFILLMENT OF THE REQUIREMENTS

FOR THE DEGREE

MASTER OF SCIENCE

DEPARTMENT OF GEOLOGY AND ENVIRONMENTAL GEOSCIENCES

Thesis Director:
Philip J. Carpenter

ACKNOWLEDGEMENTS

There are many individuals that have greatly contributed their time, expertise, and resources to this study and I would not have completed this work without their help. First, I would like to thank my parents for their support in my choosing to pursue my graduate degree and to my boyfriend for those tireless hours supporting my work and lending an open ear when I need to talk a concept out. Second, to my advisor, Phil Carpenter, who got me connected with this project and has always been there to answer questions and help guide me throughout my degree. Finally, thank you to all of the staff at the USGS who allowed me to be a part of their project and provided their time and equipment to carry out this project.

DISCLAIMER

Any use of trade, firm, or product names is for descriptive purposes only and does not imply endorsement by myself, Northern Illinois University, or the U.S. Government.

TABLE OF CONTENTS

Page

Chapter Page

LIST OF TABLES

Table Page

LIST OF FIGURES

Figure Page

LIST OF APPENDICES

Appendix Page

# CHAPTER 1

# INTRODUCTION

## Purpose and Scope

The main objective of this study was to measure the ground vibrations produced by an 80 $in^3$ (1.31 L) water gun and determine if they could potentially cause any damage to the Chicago Sanitary and Ship Canal in Lemont, Illinois and to structures along the canal. Both shallow and deep borehole geophones, along with surface geophones, were used to measure the ground vibrations at various locations and depths. Please note English units are used throughout this work at the request of the sponsors, the U.S. Geological Survey (USGS) and the U.S. Army Corps of Engineers (USACE).

## Site Description

The study area is located in Cook County, Illinois, just east of the southeast border of DuPage County (NW ¼, SE ¼, Section 15, T37N R11E, Sag Bridge Quadrangle), and is located on the north side of the Chicago Sanitary and Ship Canal (CSSC). The Cook County-DuPage County line is within 100 yards (91

m) of the site. The construction of the CSSC in 1910 connected the Chicago and Des Plaines Rivers (Figure 1) allowing for open flow of water away from Lake Michigan to the Mississippi River. Besides reversing the flow of water out of Lake Michigan and allowing for cleaner drinking water for the Chicagoland area, the CSSC creates a passageway for commercial and recreational navigation (Moy et al., 2011). This connection, and the resulting improved water quality, allowed for non-native aquatic species, like the round goby, sea lamprey, and zebra mussel, to spread throughout the connecting waterways into the Great Lakes. Various types of Asian carp are also poised to invade the Great Lakes through this waterway.

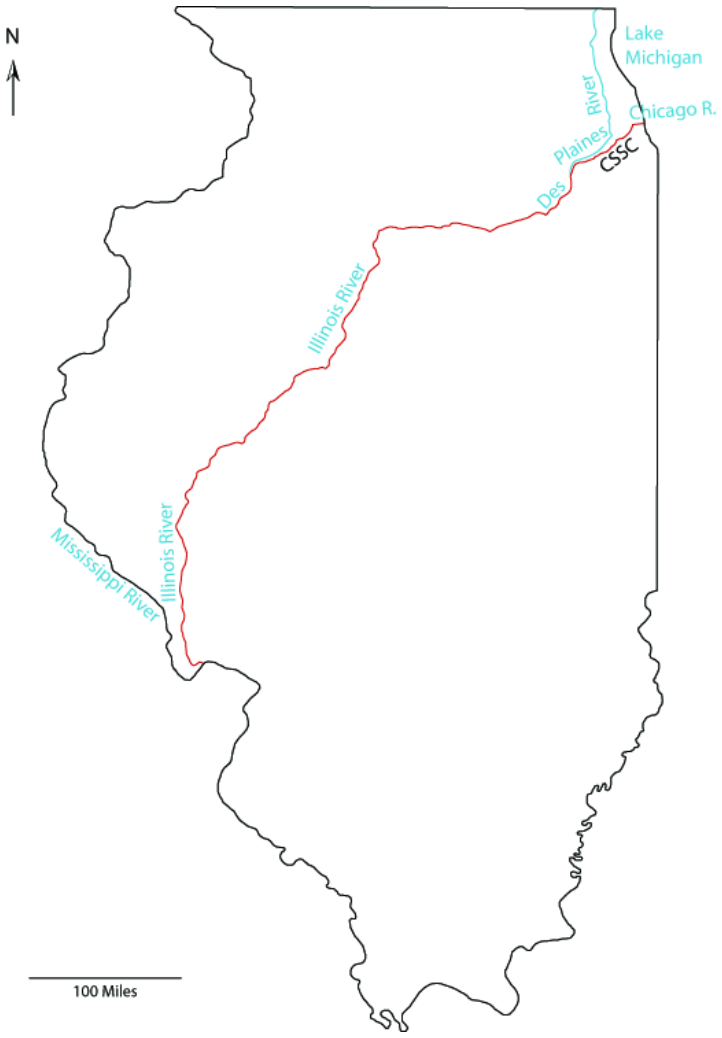


**Figure 1. Map of Illinois Showing how the CSSC allows for the connection of the Mississippi River and Lake Michigan.**

## Geological and Hydrogeological Setting

The study area lies on the eastern flank of the Wisconsin arch and the western flank of the Michigan basin. Silurian-aged silty dolomite, roughly 175 ft (53 m) thick, comprise the bedrock beneath the study site. The rocks dip gently to the east and southeast and the top of the bedrock can be found at, or near, the surface. Two major joint systems are found throughout the dolomite and play an important role in the hydrology of the area by forming an unconfined aquifer for Cook County. This aquifer is recharged locally and from precipitation through the thin overlying glacial deposits (Leetaru et al., 2004). Since the porosity and permeability of the rock are mainly due to these fractures and dissolution features, the aquifer does not have the capacity to support municipal water wells. Instead, municipal wells are usually drilled into the deeper lower Ordovician sandstone units (e.g. St. Peter Sandstone). Unconsolidated glacial till and alluvial silt and sand deposits (Zeizel et al., 1962) cover the Silurian dolomite in areas where bedrock is not at the surface (Leetaru et al., 2004). The Des Plaines River flows in the valley of a large ancient glacial river that drained portions of the Great Lakes. The floor of this valley has been considerably altered by the construction of the Illinois and Michigan Canal and Chicago Sanitary and Ship Canal, which now diverts portions of the postglacial Des Plaines River (Bretz, 1955).

# Seismic Refraction Surveys

As part of the Illinois superconducting supercollider proposal (SSC), seismic refraction surveys near the study area were conducted over various materials to determine their P-wave velocities. Some of these materials included glacial drift and outwash, alluvial deposits, sandstone, and carbonate bedrock. The closest borehole to the Lemont study site was about 10 miles (16 km) away. There, the Silurian dolomite was determined to have a velocity of about 16,000 ft/s (4880 m/s) (Heigold, 1990). Refraction experiments from 2011 at the gauging station 0.5 miles (0.8km) northeast of the survey site provided similar results with a Silurian bedrock velocity of 20,000 ft/s (6100 m/s) recorded at this location. Since the 2011 refraction experiments are so close to the study area, 20,000 ft/s (6100 m/s) would be a better representation of the canal dolomite velocity than a regionally averaged velocity of 18,000 ft/s (4800 m/s). Thus, for the purposes of this paper, a dolomite velocity of 20,000 ft/s (6100 m/s) was used for the estimation of incidence and refraction angles for the water-dolomite interface in the discussion section (Chapter 4).

# Asian Carp and the Great Lakes

Asian carp are one of the most problematic invasive species. These include grass carp (*Ctenopharyngodon idella*), black carp (*Mylopharyngodon piceus*), bighead carp (*Hypophthalmichthys*), and silver carp (*Hypophthalmichthys molitrix*) (Figure 2). Asian carps were introduced to the United States in the 1960s and 1970s as an attractive and environmentally friendly biological alternative to chemical methods for controlling weeds, other aquatic pests (Kelly et al., 2006), and for improving the water quality in wastewater treatment ponds (Chapman and Hoff, 2006). Stocking of Asian carp in open water systems and flooding of wastewater treatment ponds are the most likely Asian carp escape routes into the Mississippi River system (Kelly et al., 2011). Asian carp have already been found in Lake Erie, Lake Huron, Lake Ontario (Cudmore and Mandrak, 2011), as well as in the Mississippi River. Presently, bighead and silver carp (Figure 2 c and d) threaten to invade Lake Michigan; however, grass and black carp won't be far behind (Sparks et al., 2010). Invading Asian carp cause substantial ecological and economic damage (Mandrak and Cudmore, 2004; Nico et al. 2005; Thomas et al., 2011) by competing for food and habitat with native fish and other animals, lowering the water quality (Kolar et al., 2007), uprooting or consuming aquatic vegetation (Koel et al., 2000), and having a tendency to leap out of the water in response to passing motorboats causing possible harm to boaters and equipment.

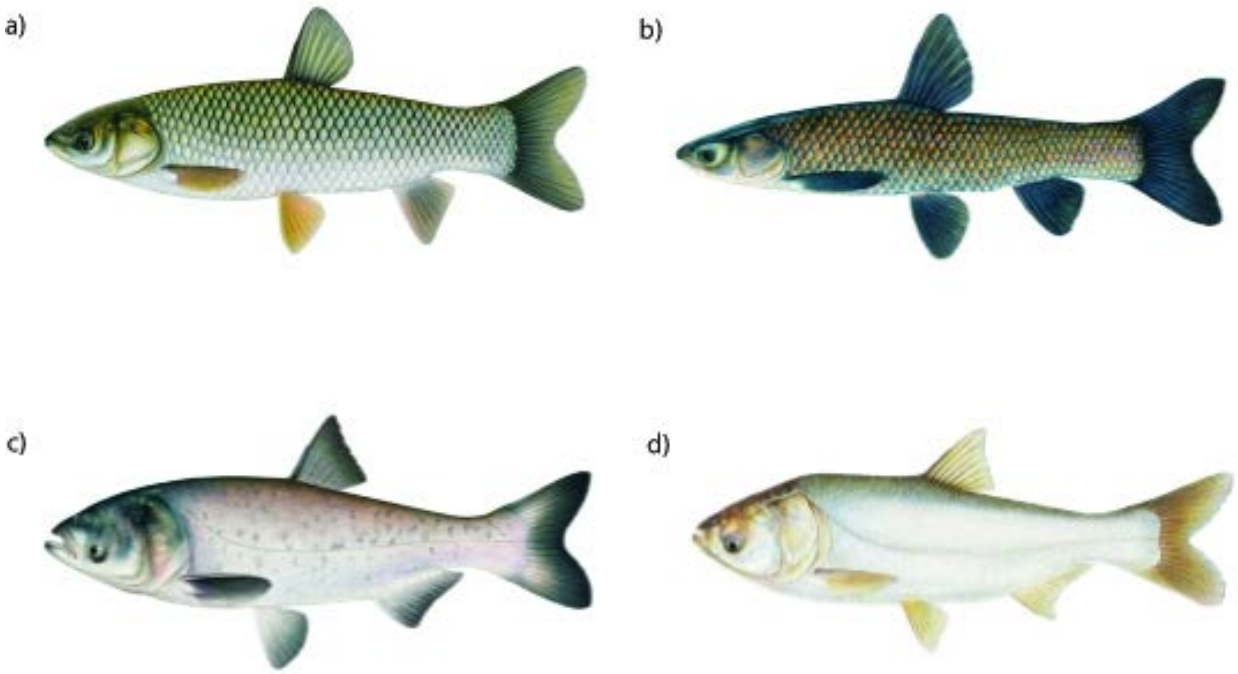


**Figure 2. Asian carp species that are invading North American waterways include a) grass carp, b) black carp, c) bighead carp, and d) silver carp.**

Control and containment (retrospectively evaluated by Britton et al., 2011) by use of a barrier has been suggested as the best method of controlling non-native species. Several barrier methods were proposed to prevent Asian carp from reaching Lake Michigan, including water filtration, ultraviolet light, heating, electricity, an electromagnetic field, bubble screens, acoustic arrays, low dissolved oxygen zones, habitat alteration, operational flow changes, and chemicals. Ultimately, a micro-pulsed DC electric array was chosen on the basis of cost, likelihood of success, minimal environmental impact, commercial availability, fewer permit requirements, and minimal effect on existing uses of the canal (Moy et al., 2011). An experimental barrier was erected and put into operation in April 2002, followed by a stronger, more permanent barrier, in April 2009 (Figure 3)**.**

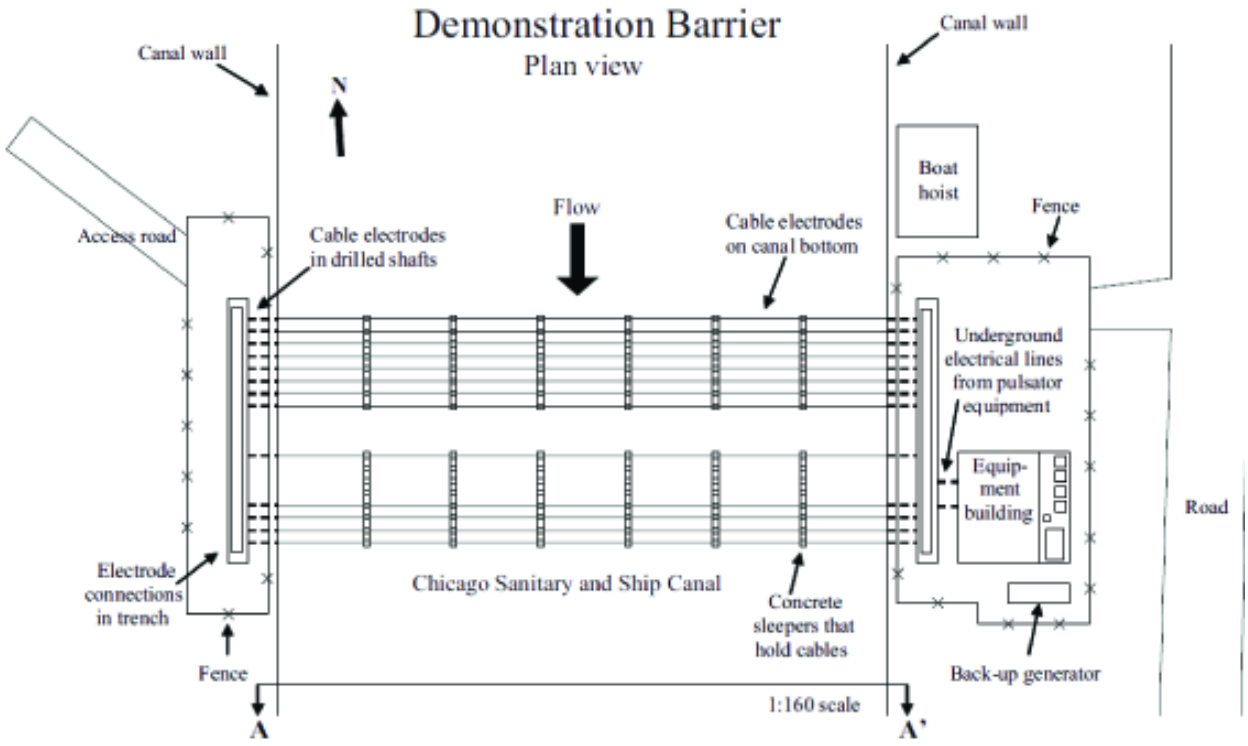


**Figure 3. Plan view of the CSSC 2002 demonstration Barrier (Moy et al., 2011). The existing barrier is a larger version of this with multiple electrode banks.**

Studies of the barrier on common carp (*Cyprinus carpio*) showed several possible issues in its efficacy. Some of these issues include equipment failure, the barrier's ineffectiveness on smaller fish, movement of the fish upstream past the barrier by external transport (fishing, biological sampling, or barge tanks), weakening of the barrier's electric field as barges pass through, and the increased conductivity of the water diminishing the effectiveness of the barrier (Sparks et al. 2010; Moy, et al., 2011). The validity of using common carp to predict Asian carp responses is also questionable. Over its lifetime the electric barrier has seen five brief disruptions in operation with the longest lasting 56 hrs (Moy et al., 2011). Due to these concerns and the fact that the DC barrier must undergo routine maintenance, another barrier method is needed to help prevent the migration of Asian carp into Lake Michigan.

## Asian Carp Water Gun (the “Carp Cannon”)

The effects of using air guns and water guns on marine life have been extensively studied by the seismic industry, primarily related to offshore oil and gas exploration. Exposed fish showed a startle response to air or water gun discharge (Boeger et al., 2006; Gordon et al., 2004; Hirst and Rodhouse, 2000). However, they begin to be less disturbed after repeated exposure (Boeger et al., 2006). Most of these studies were performed in open water so fish responses to the water gun pulses in the more confined setting of the CSSC may differ significantly. The effect of a water gun on Asian carp in the CSSC is currently being researched (Morrow et al., 2015). A water gun was chosen over an air gun because it is an implosive seismic source producing a bubble-free pulse compared to air guns which are plagued with multiple bubble pulses that could prolong and enhance ground vibrations; water guns are also less expensive than air guns (Figure 4).

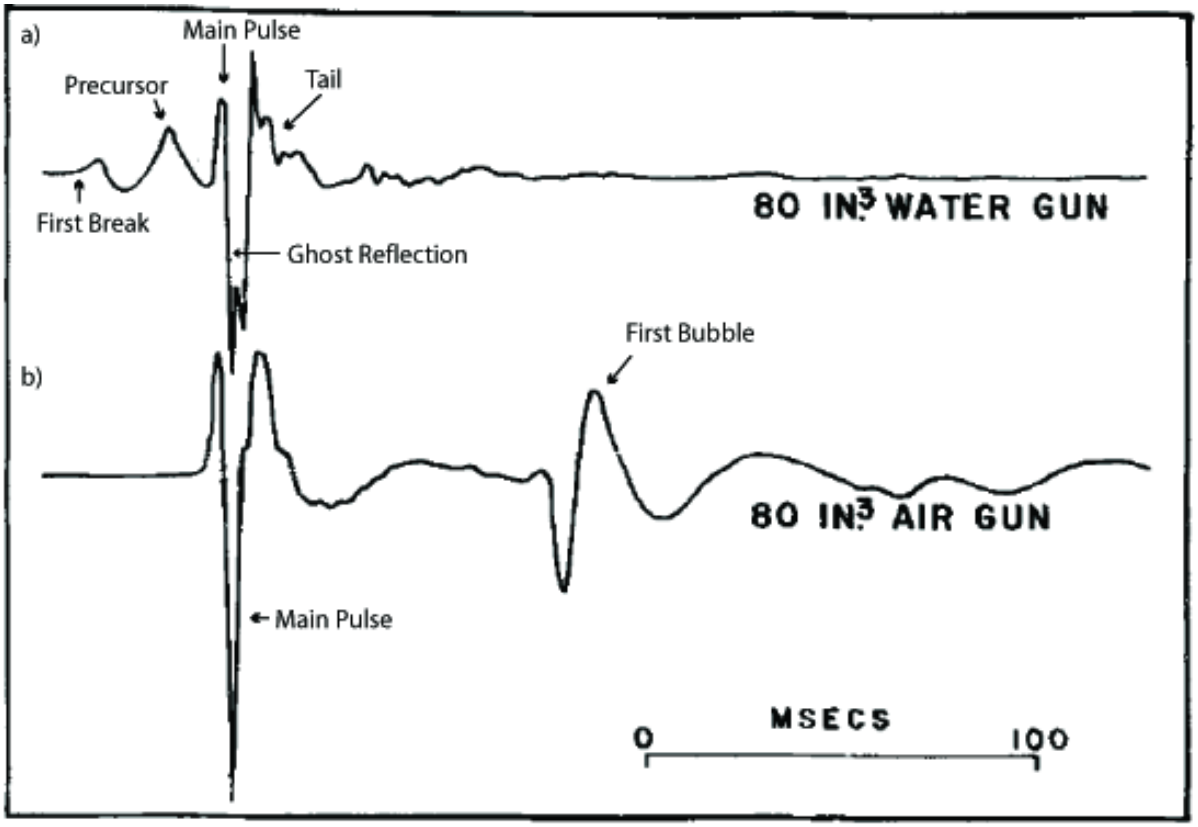


**Figure 4. A comparison between the seismic wavelet shapes of an a) 80 cu in water gun and b) an 80 cu in air gun (modified from Hutchinson and Detrick, 1984; Hutchinson, 1984). Water pressure wavelet is shown.**

A water gun has a dual chamber so that high pressure air in the upper chamber fires the piston into the lower chamber, ejecting the water through ports on both sides at the base of the gun. A cavity is formed behind the expelled water creating an implosion due to the surrounding hydrostatic pressure. This implosion produces the main pulse of the water gun's seismic signature (Figure 5) (Hutchinson, 1984), shortly followed by a "ghost" reflection, which is a reflection off the water-air interface at the surface.

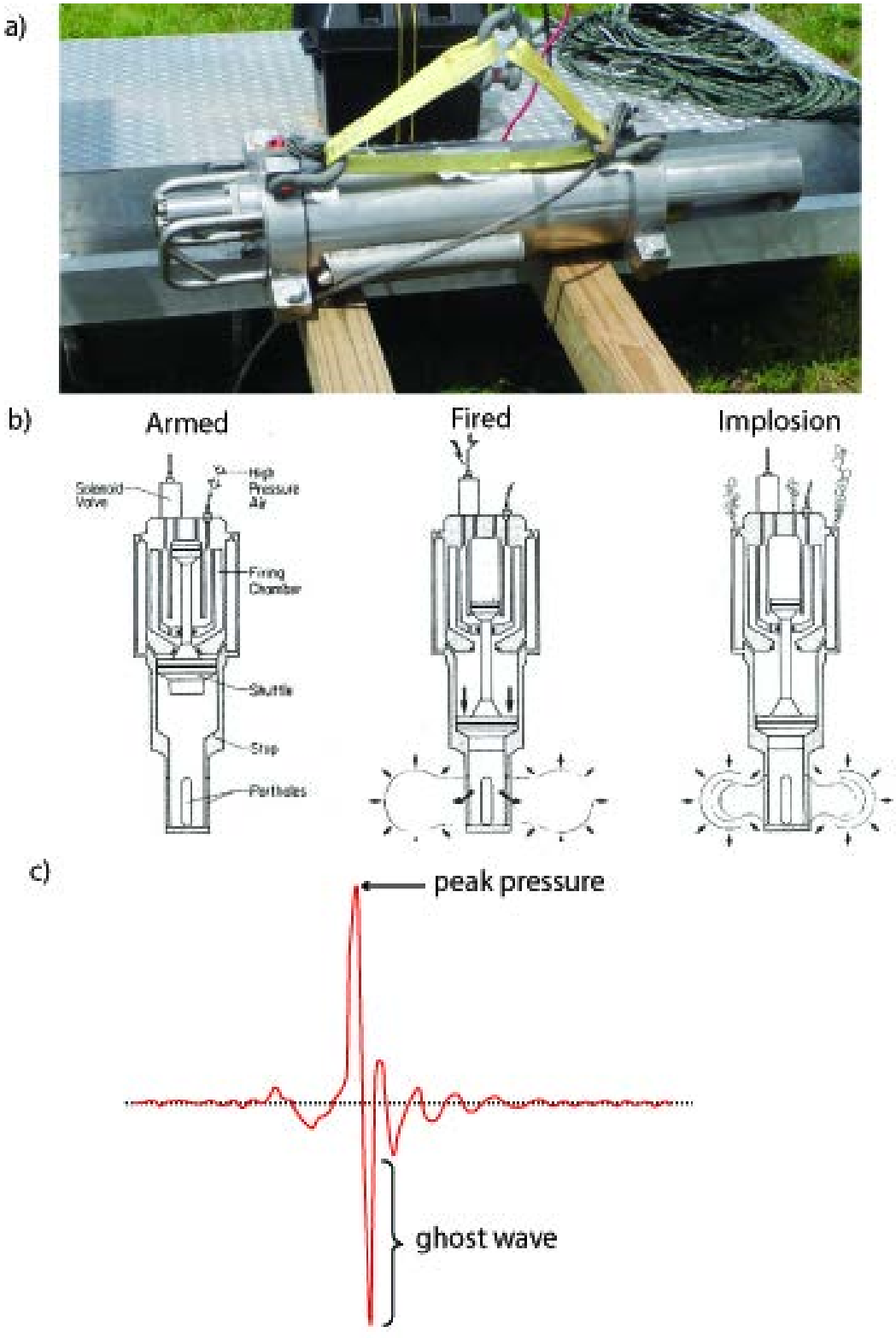


**Figure 5. a) Bolt Model P400 80 in³ (1.3 L) water gun, b) what happens when a water gun is fired (Hutchinson, 1984), and c) the idealized water gun pressure pulse recorded.**

The seismic waves recorded on shore produced by the firing of a water gun consist initially of P-waves (aka compressional or longitudinal waves) and S-waves (shear or transverse waves). Since the water gun will be fired in water, the seismic energy will be partitioned at the water-canal interface because the materials have different seismic velocities, 5,000 ft/s (1524 m/s) and approximately 20,000 ft/s (6100 m/s) respectively. S-waves cannot travel through water so the P-waves must convert to SH (shear horizontal) and SV (shear vertical) at the canal wall or canal bottom (Lillie, 1999). A simplified view of seismic ray travel paths for the direct, reflected, and critically refracted P-waves is shown in (Figure 6).

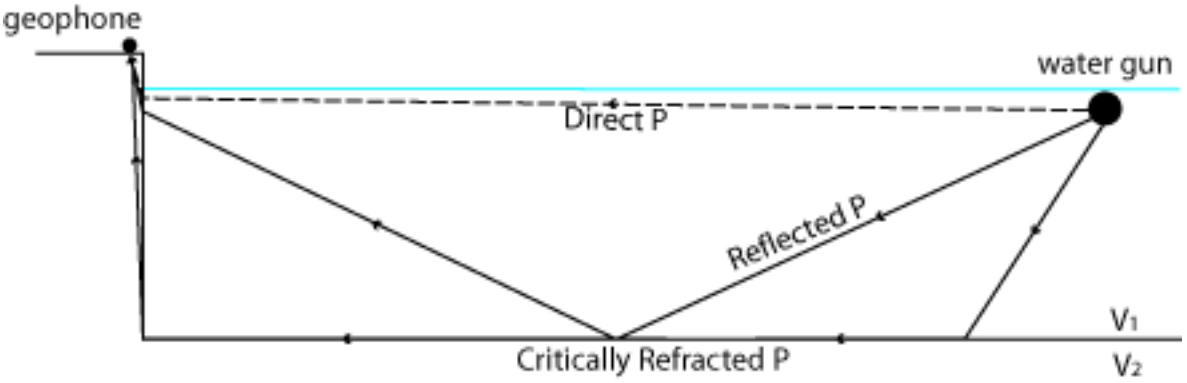


**Figure 6: Ray paths for the direct, reflected, and critically refracted P-wave for a water gun shot in the CSSC arriving at a receiver at or near the canal wall (modified from Lillie, 1999). Note the direct P-wave also undergoes refraction at the canal wall. The horizontal blue line is the water surface.**

## Sensors

Geophones are the recording instruments used to measure ground movement produced by seismic sources. They consist of a magnet suspended by springs within a coil of wire. Movement of the springs and magnet produces an electrical current and voltage (Lillie, 1999); the voltage is proportional to ground velocity (also called particle velocity). They have the ability to measure ground movement in up to

three directions (transverse, longitudinal, and vertical). The geophones are stuck into the ground using three metal prongs or attached to a borehole wall using a leaf spring.

The R.T. Clark® 3C-10 Hz geophones consist of three orthogonally mounted identical 10 Hz natural frequency geophones. Each geophone has the same response shown in Figure 7. Frequency vs. amplitude was chosen in Geopsy® when analyzing a shot to display the frequency spectrum of each wavelet. Amplitude in this case, however, represents ground velocity. More than 75% of the frequencies recorded at Lemont were greater than 40 Hz and there are no frequency peaks less than 30 Hz (Figure 8). These spectra were from a 2000 psi (13.8 MPa) shot located 30 ft (9.1 m) from the canal wall and recorded by the surface geophone located next to the 5 and 35 ft (1.5 m and 10.7 m) boreholes. These values fall in the flat response portion of geophone response spectrum (Figure 7), allowing for a simple conversion from mV to in/s or millimeters/s (mm/s). The following calculates the conversion from millivolts (mV) to ground velocity in inches per second (in/s):

Using the geophone sensitivity of 27.5 V/m/s:

$$27.5\,V = 1\,\frac{m}{s},$$

$$1\,V = 0.0364\,\frac{m}{s},$$

$$1\,mV = 3.64x10^{-5}\,\frac{m}{s} = 0.0364\,mm/s,$$

$$1\,mV = 3.64x10^{-5}\,\frac{m}{s}\left(39.4\,\frac{in}{m}\right) = 0.00143\,\frac{in}{s},$$

$$1\,mV = 1.43x10^{-3}\,\frac{in}{s}.$$

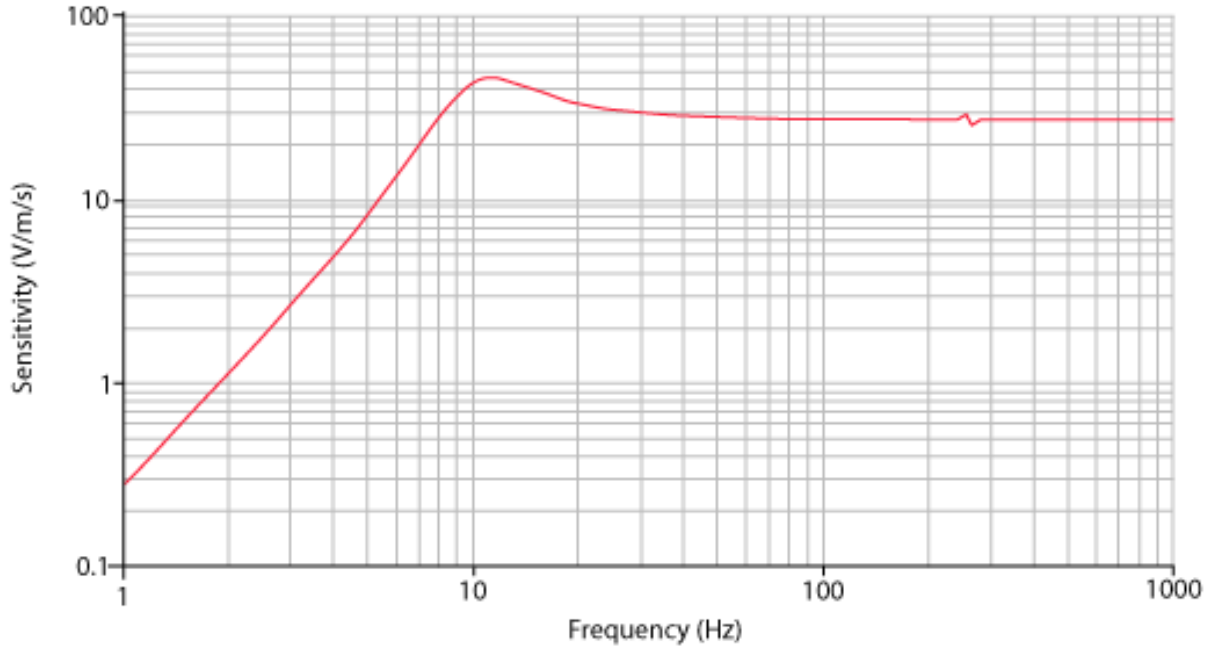


**Figure 7. Response spectrum for an R.T. Clark® 10 Hz geophone with a laveled sensitivity of 27.5 V/m/s.**

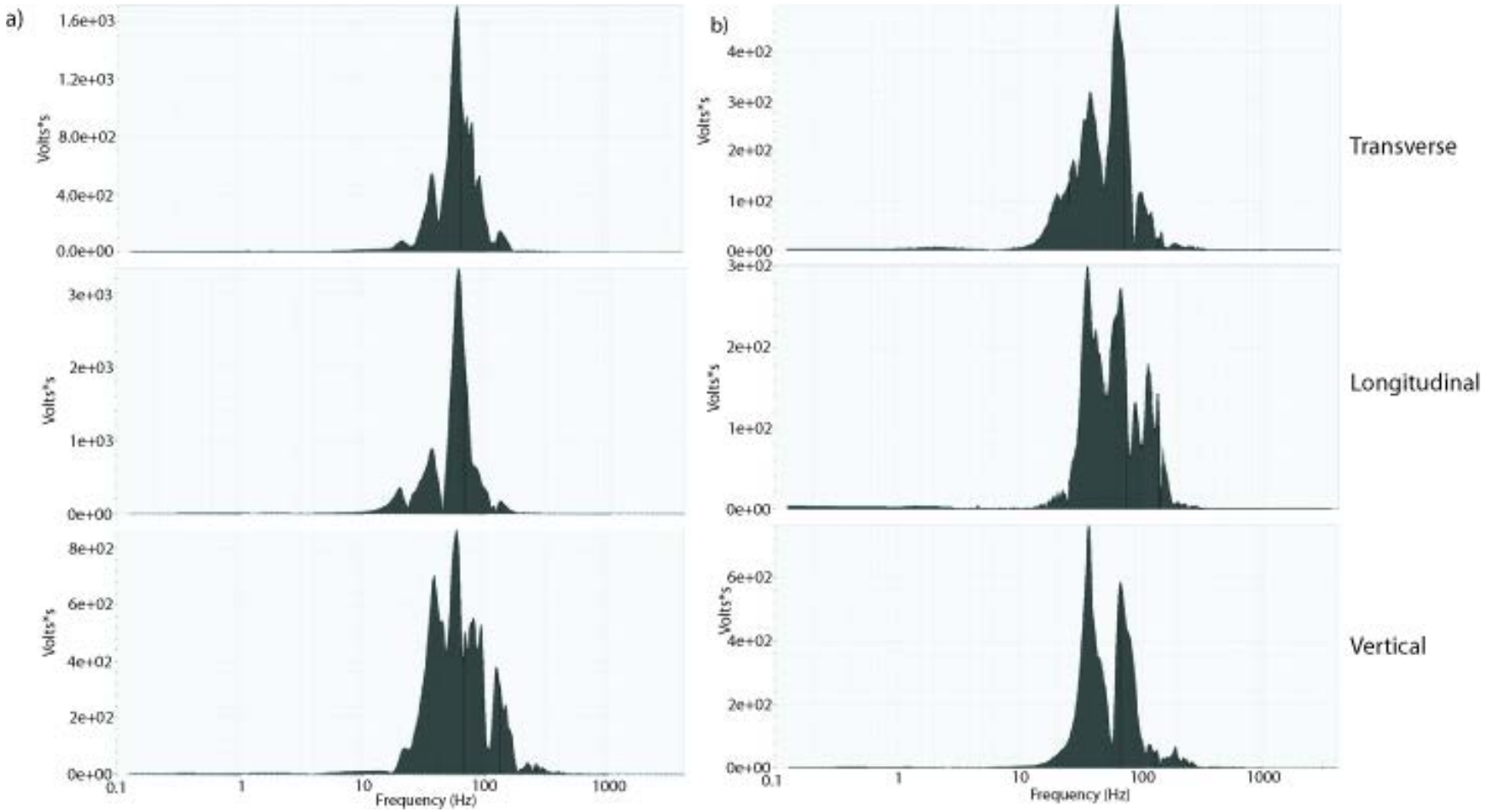


**Figure 8. Frequency spectrum for all three components of the a) 5 ft (1.5 m) red and b) 35 ft (10.7 m) blue surface geophones from a 2000 psi (13.8 MPa) shot located 30 ft (9.1 m) from the canal wall.**

## Total Vector-Sum Ground Velocity

The maximum ground vibration felt by the canal wall does not come from just one component but from the interaction of all peak values of the three components (transverse, longitudinal, and vertical). This ground vibration value is known as the peak sum vector (Dowding, 1985). This value can be calculated by using the equation from Dowding (1985), in which u is displacement:

$$\text{peak vector sum} = \sqrt{\mathring{u}_R^2 + \mathring{u}_V^2 + \mathring{u}_T^2} \qquad (1)$$

where $\mathring{u}_R$is the ground vibration (velocity) in the longitudinal direction, $\mathring{u}_V$is the ground vibration in the vertical direction, and $\mathring{u}_T$is the ground vibration in the transverse direction. The use of vector sum is somewhat controversial due to the common practice of choosing peak velocity values from different parts of a waveform (Dowding, 1985). It does, however, provide an additional margin of safety, since vector sum values are somewhat higher than single-component peak velocity values. In this study great care was taken to insure vector sum velocities were computed from the same part of the wavelet.

# CHAPTER 2

# METHODS

## Study Site

Lemont, Illinois (41.686216°N, -87.979243°W) is a southwest suburb of Chicago about 35 minutes from downtown Chicago. The CSSC runs east-northwest through Lemont, parallel with the Des Plaines River. The testing site is located on the north side of the canal approximately 1.25 miles (2.0 km) northeast of the intersection of Lemont Road/State Street and the CSSC (Figure 9). This location was chosen because a similar water gun experiment had previously been carried out there in 2011. Geophone saturation in the 2011 experiment caused clipping of the data so the true peak ground velocity could not be recorded (Morrow et al., 2015); thus the 2011 experiments had to be repeated. At this point, the canal is approximately 167 ft (51 m) wide and 25 ft (7.6 m) deep with walls comprised of emplaced dolomite blocks (Morrow et al., 2015).

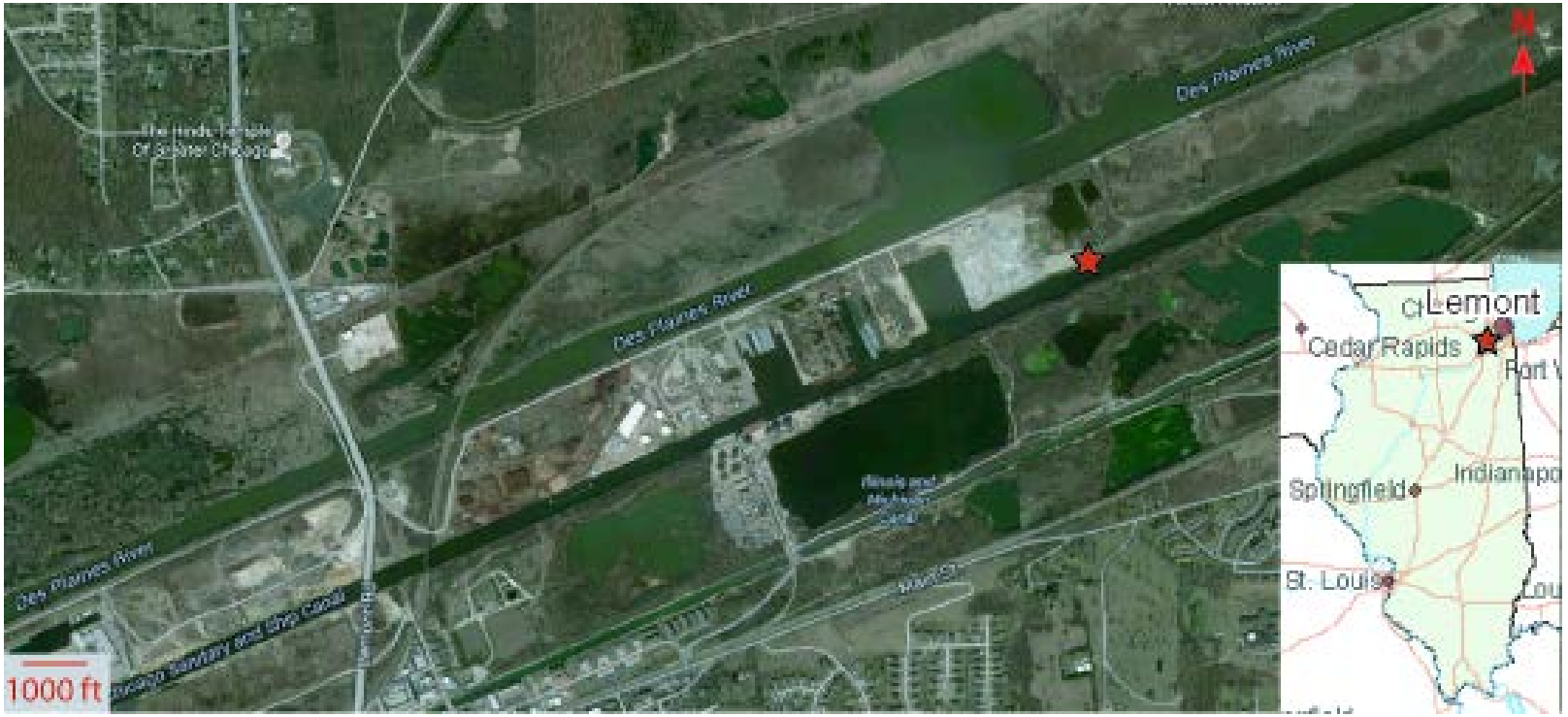


**Figure 9. Survey site location (red star) along the CSSC in Lemont, Illinois.**

# Experimental Design

Due to outside experimental constraints, only the geophone arrangements were able to be changed during this survey, within a very small area. All water gun locations, water gun depths, and shot pressures were predetermined and controlled by the USGS and USACE.

## Experiment 1

A series of 4 inch (10.2 cm) diameter boreholes were previously drilled 5, 35 and 100 ft (1.5, 10.7 and 30.5 m) away from the canal wall to the approximate depth of the bottom of the canal (~35 ft or 10.7 m below ground surface). Two R.T. Clark® 10 Hz downhole 3-component geophones with a resistance of 395 ohms and sensitivity of 27.5 V/m/s were placed down each borehole, one shallow and one deep, and affixed to the borehole wall using spring clamps. The shallow geophone was suspended 5 ft (1.5 m) below the ground surface (bgs) in all of the boreholes while the deep geophone was suspended 25 ft (7.6 m) bgs in the 35 and 100 ft (10.7 and 30.5 m) boreholes and 20 ft (6.1 m) bgs in the 5 ft (1.5 m) borehole (Figure 10a). The difference in deep geophone depth for the 5 ft (1.5 m) borehole is to account for the elevation difference at that point so that the deep geophones were all suspended at about the same elevation as the water gun. No topographic adjustments were made for the shallow geophones between the boreholes. Tap tests were administered in order to determine the orientation of the horizontal components of the borehole geophones but were unsuccessful. Two R.T. Clark® 10 Hz 3-component surface geophones with a resistance of 395 ohms and a sensitivity of 27.5 V/m/s were placed next to the

5 and 35 ft (1.5 and 10.7 m) boreholes (Figure 11). The pointed end of the geophone was placed facing away from the canal. This made the transverse component (channel 1) parallel with the canal wall (east-west) and the longitudinal component (channel 2) perpendicular (north-south) with the canal wall. The vertical component (channel 3) remains up and down.

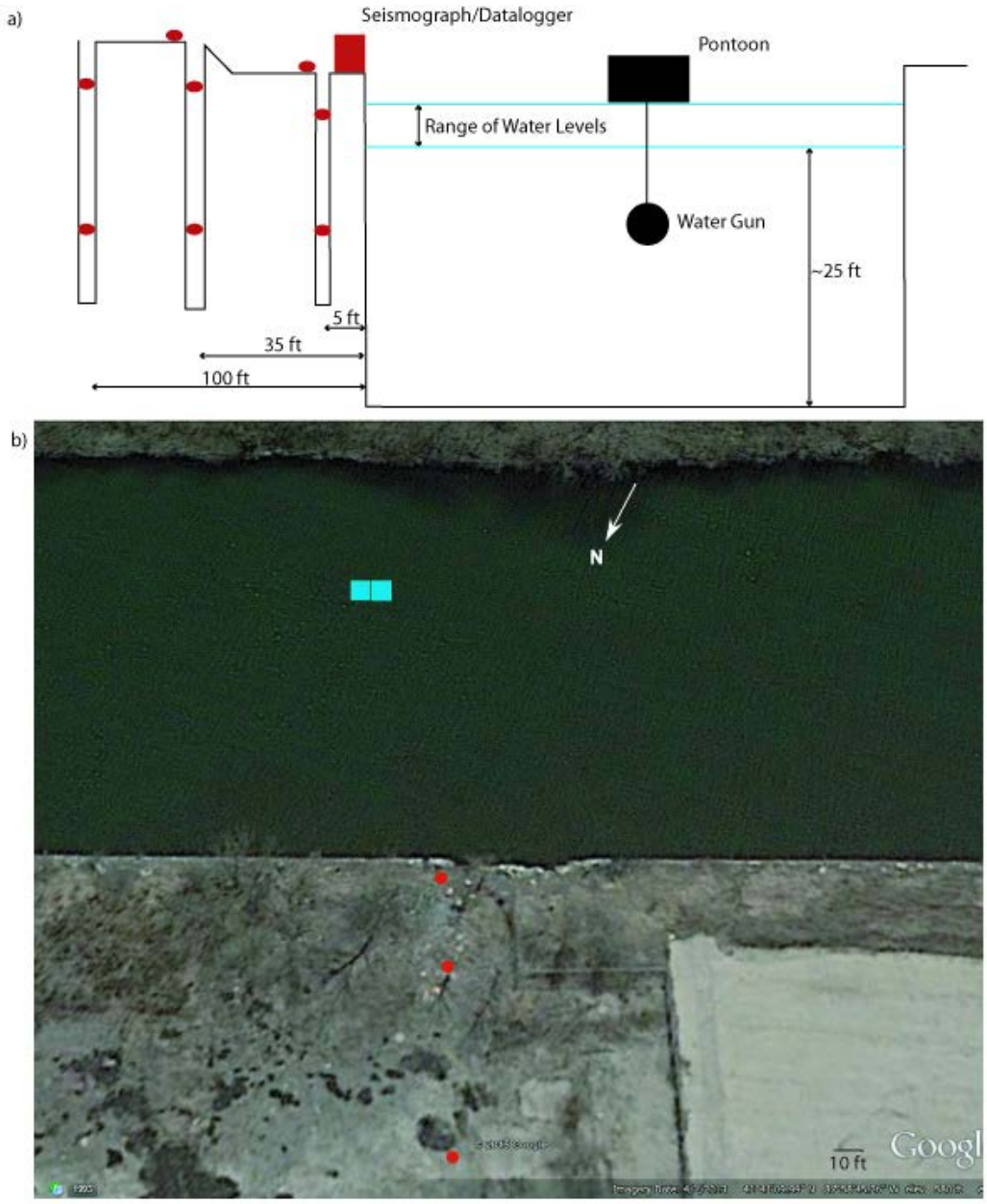


**Figure 10. a) First geophone layout (red dots) and experiment setup at the survey site, not to scale (modified from Morrow et al., 2015). b) Shots were offset from the geophones by about 30 ft (9.1 m).**

**Figure 11. Surface geophone position next to the 5 ft (1.5 m) from the canal wall with downhole geophone cables.**

Two Bolt® Model P400 80 in³ (1.31 L) water guns were mounted to separate pontoon boats and offset from the geophones 15 ft (4.6 m) upstream (Figure 10b). Water gun #1 was suspended at a depth of 14 ft (4.3 m) into the water while water gun #2 was suspended 4 ft (1.2 m). Both guns are aligned parallel with the canal so that the ports faced the canal wall (Figure 12). Fifteen shots were taken at 2000 psi (13.8 MPa) 30, 40, 50, 60, 70, 80, and 90 ft (9.1, 12.2, 15.2, 18.3, 21.3, 24.4, and 27.4 m) from the canal wall (five with gun #1, five with gun #2, and five with both guns). The water guns were not fired any closer to the canal at the request of USACE.

**Figure 12. Water guns suspended from pontoon boats in the middle of the canal.**

Data were collected using a Geometrics Geode® 24-channel seismograph with no filters, no preamplifier gain, and normalized display gain to ensure no clipping (saturation) of the data. A sample interval of 0.125 ms for 8 s was used while collecting data. All of the geophones were channeled through routing switchboxes to the Geode® seismograph which then digitized and recorded all the signals. Data were then downloaded to a Panasonic Toughbook personal computer running Windows-7. The program used to run the seismograph and record the data was the Geometrics Seismodule Controller® (Version 11.1.69.0).

## Experiment 2

A second somewhat different layout was used in Experiment 2. In this new layout, four geophones were laid out in a line with 10 ft (3.05 m) separation between geophones (Figure 13). The two water guns were still oriented parallel with the canal but this time were each placed 40 ft (12.2 m) from the canal walls with an 80 ft (24.4 m) separation between them and lowered to a depth of 14 ft (4.3 m) below the water surface. Gun #1 was on the north side of the canal while gun #2 was on the south side of the canal. The water guns were aligned with the middle of the geophone array (between the white and green geophones) line so that there was a 5 ft (1.5 m) lateral offset from the closest geophones (white and green). A series of 10 shots, five with gun #1 and five with both, were made at 2000 psi (13.8 MPa). Data were recorded using the same equipment and sampling interval as in Experiment 1. The purpose of this second experiment was to compare the differences between ground vibrations in-line and offset from a water gun shot.

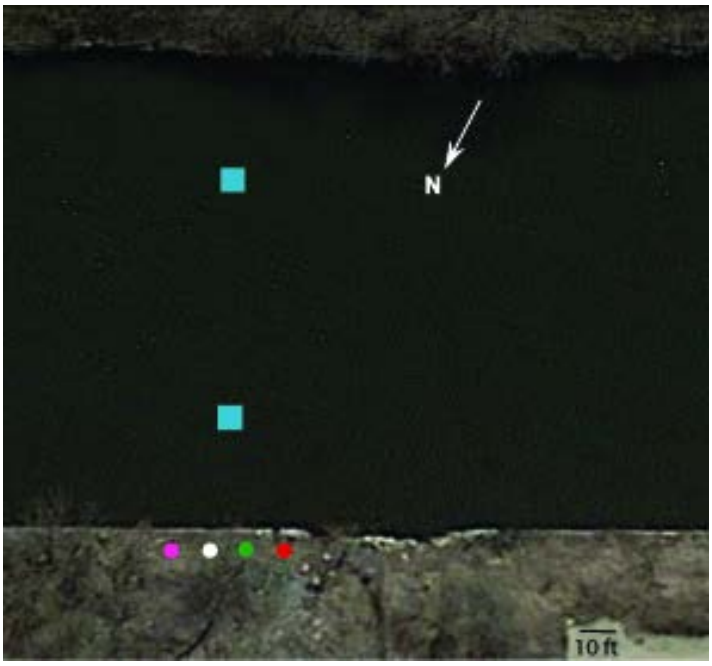


**Figure 13. Water gun and geophone configuration for experiment 2**

## Experiment 3

A third layout used the same water gun configuration as experiment 2 but with water guns shooting at 1000 psi (6.9 MPa) and a grid geophone layout (Figure 14). The water guns were centered in the middle of the grid so that they were offset 5 ft (1.5 m) from the closest geophones. The purpose of this experiment was to duplicate the layout previously used at Brandon Road Lock and Dam so that comparisons could be made to the Brandon Road data set. Again, data were recorded using the same equipment and sampling interval as in the previous two experiments.

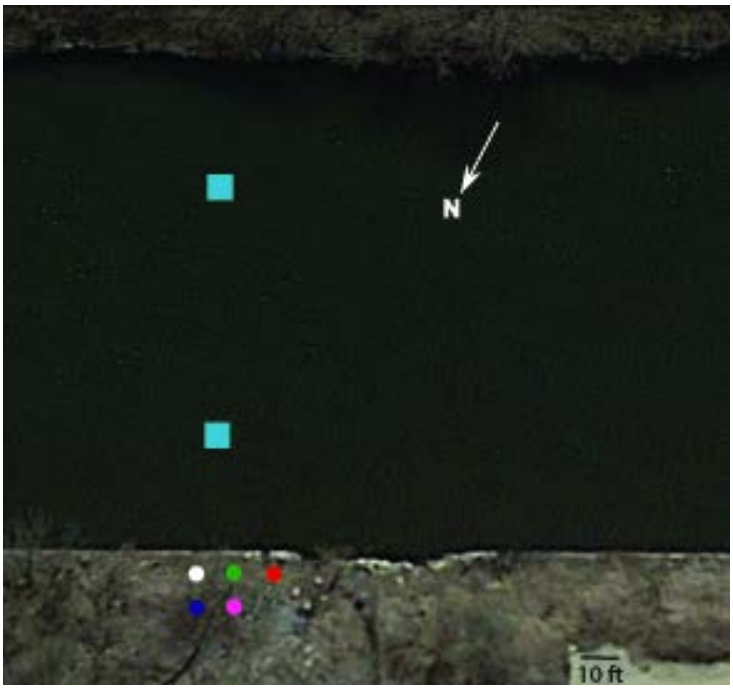


**Figure 14. Water gun and geophone configuration for experiment 3**

# Data Analysis Methods

Using Geopsy® (Version 2.7.0), individual channels' wavelets can be analyzed to see where in the wavelet the maximum amplitude occurs. This also gives a rough estimate of the maximum voltage values for each channel. The voltages are then extracted from Geopsy® in ASCII format to be further analyzed in Microsoft Excel, specifically to identify a maximum voltage or ground motion (either positive or negative), or a specific channel's wavelet was examined in more detail in Global Earthquake Explorer® (Version 2.2.0). The voltage of each component (vertical, north-south, and east-west) were sorted by maximum voltage and visually examined to analyze whether they occur at the same time on the wavelet.

To determine a relationship between maximum ground velocities and increasing shot distance, the vertical component of the red and blue geophones was analyzed for shots taken from 30-90 ft (9.1-27.4 m). The maximum voltage values at each shot distance are averaged and graphed to determine any trends. This same analysis technique was applied to the horizontal components for shots at 30-90 ft (9.1-27.4 m) to see if the maximum voltage trends between the channels vary as shot distance increases. These values are compared to the 5 ft (1.5 m) white geophone that is more closely aligned with the water guns. Then it is possible to determine seismic wave travel paths from the water gun to the receiving geophones. To assess whether background noise has an effect on the main pulse of the water gun, the background maximum voltages are also analyzed.

Using the sum component vector equation, the total voltage felt from both the downhole and surface geophones is calculated from a shot 30 ft (9.1 m)from the canal wall at 2000 psi (13.8 MPa) to produce an overall ground vibration map of the survey area. The frequency spectra of the red and blue geophones are analyzed from the 30 ft (9.1 m) shot sequence to estimate the peak frequencies being emitted by the water gun.

# CHAPTER 3

# RESULTS

## Experiment 1: Ground Motion vs. Shot Distance

### Maximum Amplitude and Wavelet Repeatability

By comparing the recorded vertical component wavelets of the same geophone from the same shot sequence, the peak particle velocity (PPV i.e. maximum amplitude) for each shot shows that the maximum voltage always occurs as the major peak in the beginning of the wavelet (Figure 15).

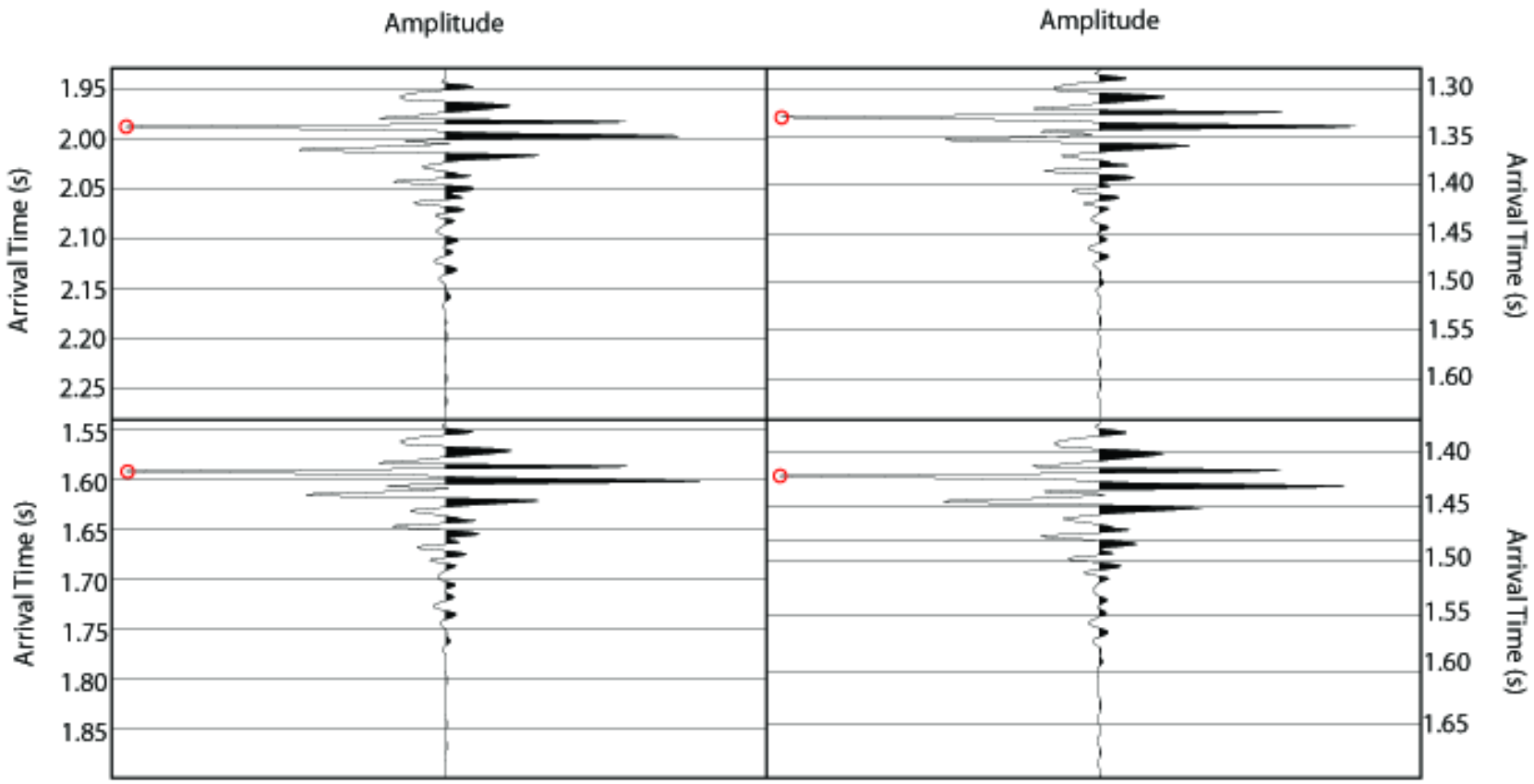


**Figure 15. Vertical component wavelets from the same shot sequence from the same geophone showing that the greatest amplitude (red circles) occur from the same point on the wavelet.**

It is also important that the maximum ground vibration of each component occurs at the same point in time. The same data was analyzed to see at what time the maximum ground vibration occurs for each component (Table 1 and Figure 16). Table 1 and Figure 16 show that the maximum ground movement of each component occurs at the same time for the shot sequence located 30 ft (9.1 m) from the canal wall shot at 2000 psi (13.8 MPa). The maximum ground vibration of the vertical component occurs slightly faster than the horizontal components. This is also seen when the wavelets are stacked on top of each other; the vertical component is shifted slightly to the left (Figure 16). This shift may be due to the seismic wave recorded by the vertical component is travelling a faster path than the seismic waves recorded by the horizontal components. The vertical component may be travelling through the water, critically refract when it hits the bottom of the canal, travel along the bottom of the canal, and then refract up towards the surface when it reaches the canal wall. Since the velocity of the dolomite is much greater than that of the water, a seismic wave will arrive faster, even though the travel path may be longer.

**Table1**

Maximum Ground Movement and Arrival Time

| Shot # | Transverse<br>in/s<br>(mm/s) | Arrival Time<br>(s) | Longitudinal<br>in/s<br>(mm/s) | Arrival Time<br>(s) | Vertical<br>in/s<br>(mm/s) | Arrival Time<br>(s) |
|---|---|---|---|---|---|---|
| 1 | 0.132<br>(3.35) | 2.01 | 0.218<br>(5.54) | 2.01 | 0.119<br>(3.02) | 1.99 |
| 2 | 0.136<br>(3.45) | 1.61 | 0.220<br>(5.59) | 1.61 | 0.118<br>(3.00) | 1.59 |
| 3 | 0.140<br>(3.56) | 1.35 | 0.218<br>(5.54) | 1.35 | 0.117<br>(2.97) | 1.33 |
| 4 | 0.141<br>(3.58) | 1.44 | 0.214<br>(5.44) | 1.44 | 0.117<br>(2.97) | 1.42 |
| 5 | 0.139<br>(3.53) | 1.86 | 0.214<br>(5.44) | 1.86 | 0.118<br>(3.00) | 1.84 |

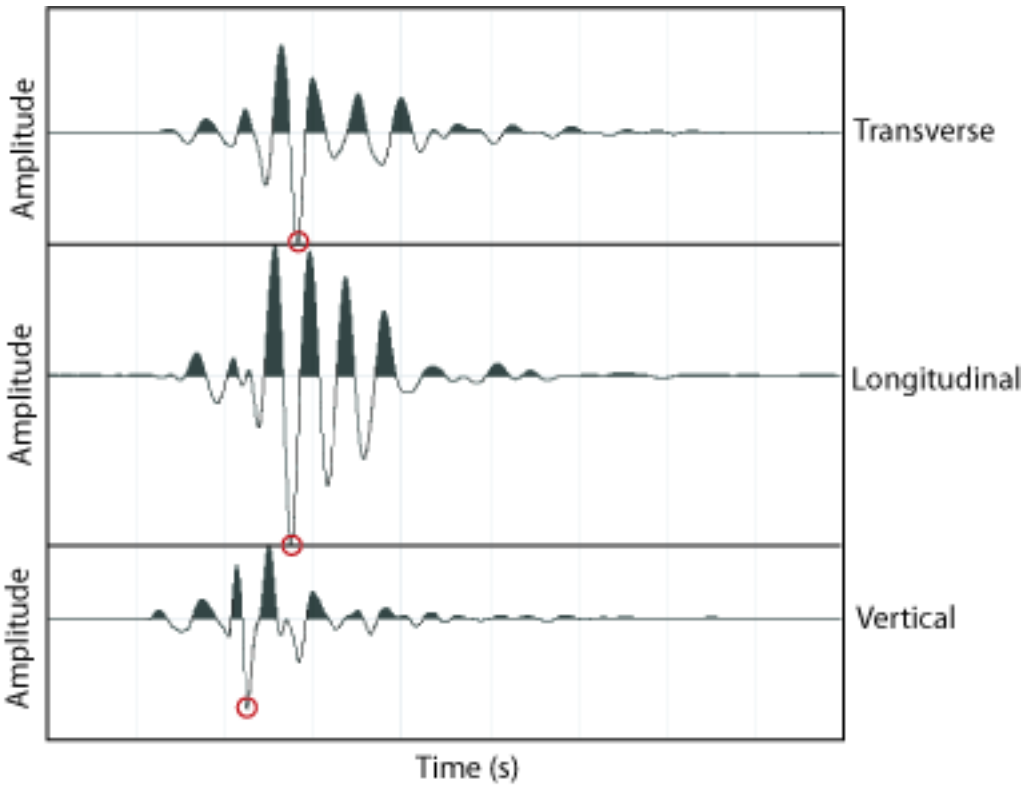


**Figure 16. Wavelets of all three components from one of the shots in Table 1 showing that the maximum ground movement for each channel occurs at the same point on the wavelet with the vertical maximum arriving earlier. Amplitude is actually the ground velocity.**

Change in Maximum Amplitude (PPV) with Increasing Shot Distance from the Canal Wall

The analysis of the change in maximum surface ground vibration (PPV) for all three components of the 5 and 35 ft (1.5 and 10.7 m) surface geophones as well as the vertical component of the downhole geophones for the 5 ft (1.5 m) borehole as a function of gun #1's shot distance from the canal wall is shown in Figure 17.

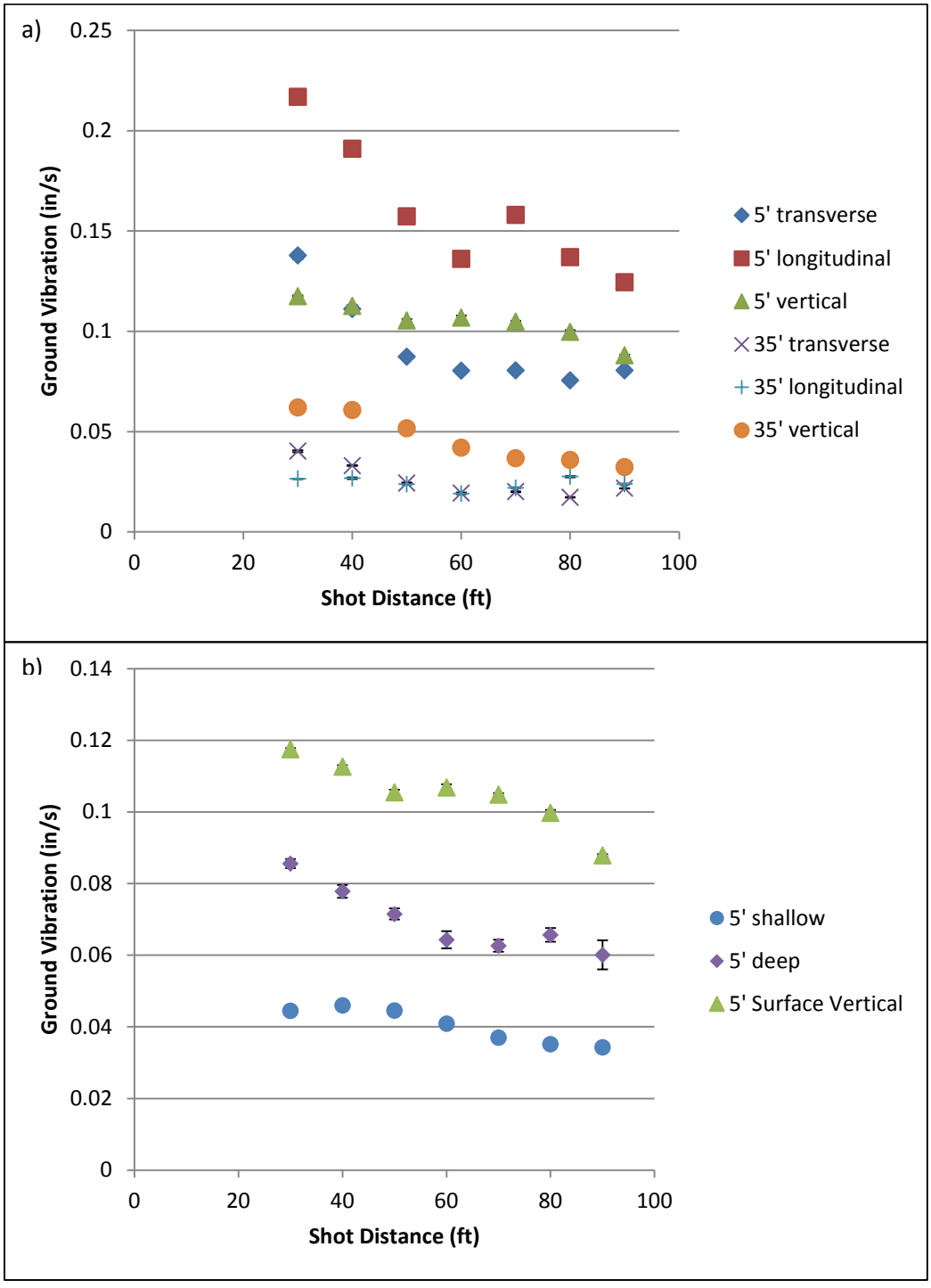


**Figure 17. a) Change in ground movement as shot distance increases for all three components from the surface geophones located 5 and 35 ft (1.5 and 10.7 m) from the canal wall, respectively. b) A comparison of the vertical component for the 5 ft (1.5 m) surface, shallow, and deep geophones as shot distance increases. Both graphs are plotted with standard error (1 standard deviation of the mean).**

## Sum Component Vector for Maximum Ground Motion

Since the 5 ft (1.5 m) from the canal surface geophones showed the largest ground motion, this geophone response was selected to compute the sum component vector of ground motion. Table 2 displays the values making up the sum component vector for the 5 ft (1.5 m) surface geophone with a shot approximately 30 ft (9.1 m) from the canal wall. The maximum ground vibration felt by the 5 ft (1.5 m) surface geophone after applying the sum component vector is 0.28 in/s (7.11 mm/s).

Table 2

Sum Component Vector Sample Calculation

| Shot # | Transverse<br>in/s<br>(mm/s) | Longitudinal<br>in/s<br>(mm/s) | Vertical<br>in/s<br>(mm/s) | Sum Component Vector<br>in/s<br>(mm/s) |
|---|---|---|---|---|
| 1 | 0.132<br>(3.35) | 0.218<br>(5.54) | 0.119<br>(3.02) | 0.281<br>(7.14) |
| 2 | 0.136<br>(3.45) | 0.220<br>(5.59) | 0.118<br>(3.00) | 0.285<br>(7.24) |
| 3 | 0.140<br>(3.56) | 0.218<br>(5.54) | 0.117<br>(2.97) | 0.285<br>(7.24) |
| 4 | 0.141<br>(3.58) | 0.214<br>(5.33) | 0.117<br>(2.97) | 0.282<br>(7.16) |
| 5 | 0.139<br>(3.53) | 0.214<br>(5.33) | 0.118<br>(3.00) | 0.281<br>(7.14) |
| mean | 0.1376<br>(3.50) | 0.2168<br>(5.51) | 0.1178<br>(2.99) | 0.283<br>(7.19) |

Using the sum component vector equation, an overall ground vibration cross-section of the survey area is shown in Figure 18. From this map, it can be seen that the largest PPV values are recorded at the top corner of the canal. There is also a strong response for the deep borehole geophone compared to the shallow borehole geophone.

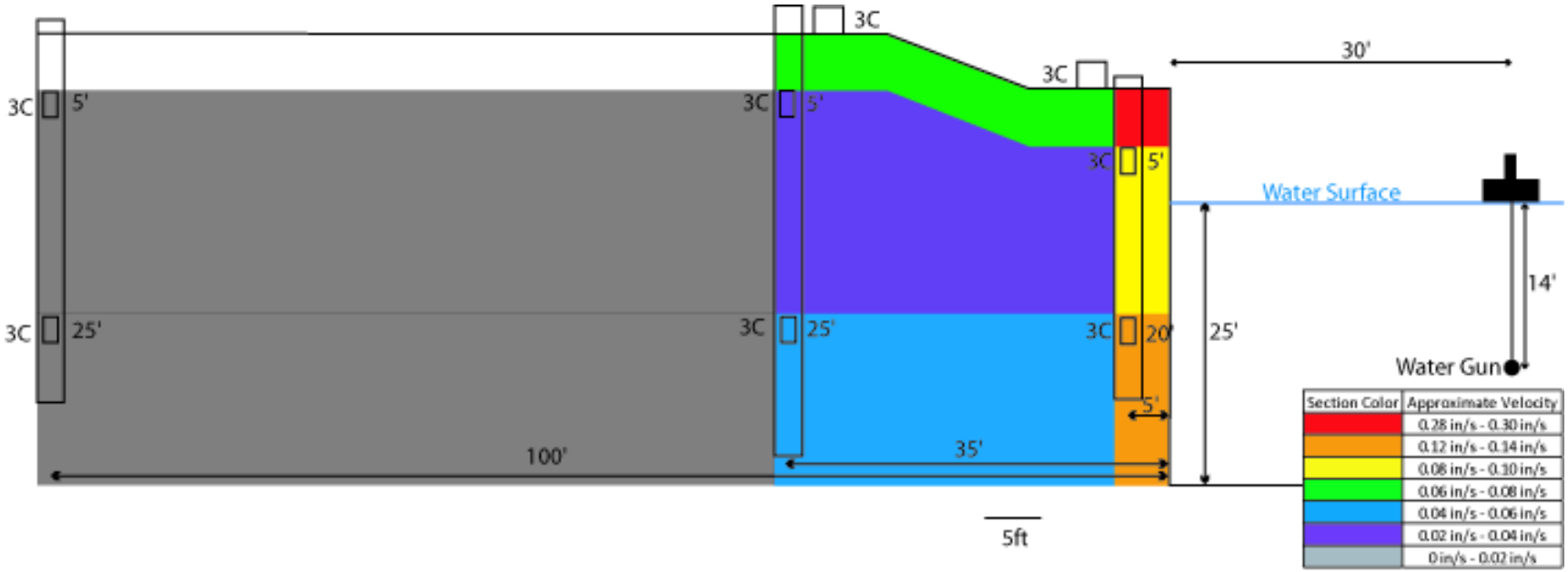


**Figure 18. Cross section showing the variation in vector sum component velocity across the survey area from a water gun shot 30 ft from the canal wall at 2000 psi (13.8 MPa). Display concept from Alonzo (2013).**

Double Gun

The wavelets and their corresponding PPVs of all three components for a double gun shot are shown in Figure 19 and Table 3. The PPVs for both the single gun shots are displayed in Table 3 as well for easier comparison.

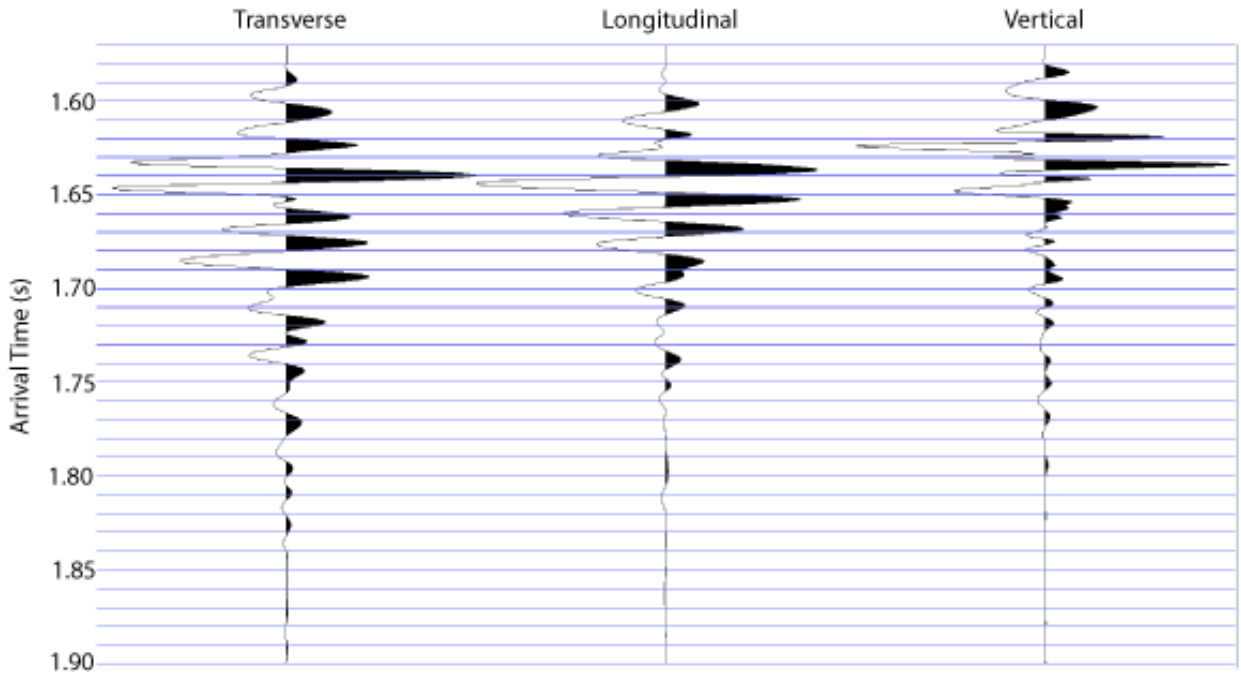


**Figure 19. Wavelets of all three components recorded at the 5 ft (1.5 m) from the canal red surface geophone from a double gun shot at 2000 psi (13.8 MPa) 30 ft (9.1m) into the canal wall.**

Table 3

Offset Geophone PPVs Produced by a Double shot

| | Transverse<br><br>in/s<br>(mm/s) | Longitudinal<br><br>in/s<br>(mm/s) | Vertical<br><br>in/s<br>(mm/s) | Sum Component Vector<br><br>in/s<br>(mm/s) |
|---|---|---|---|---|
| Both Guns | 0.08<br>(2.03) | 0.20<br>(5.08) | 0.10<br>(2.54) | 0.24<br>(6.10) |
| Gun #1 (14') | 0.14<br>(3.56) | 0.22<br>(5.59) | 0.12<br>(3.05) | 0.28<br>(7.11) |
| Gun #2 (4') | 0.05<br>(1.27) | 0.08<br>(2.03) | 0.04<br>(1.02) | 0.10<br>(2.54) |

## Frequency Content

The amplitude spectrum of an entire wavelet was generated using Geopsy® by displaying a channel's wavelet and clicking the frequency (amplitude) button. Note that amplitude here refers to ground velocity. At different shot distances the frequency of some channels varies slightly, but overall the frequency content remained relatively constant as shot distance increases. An example frequency spectrum, explained in Chapter 1, for the entire wavelet of each component of the surface geophones is displayed in Figure 8. Recorded frequencies were generally above 40 Hz. The somewhat regular peaks in the spectra suggest reverberation in the wavelet, which may also be seen near the end of the wavelets. Most likely this reverberation is from the pressure wave bouncing back and forth between the canal walls.

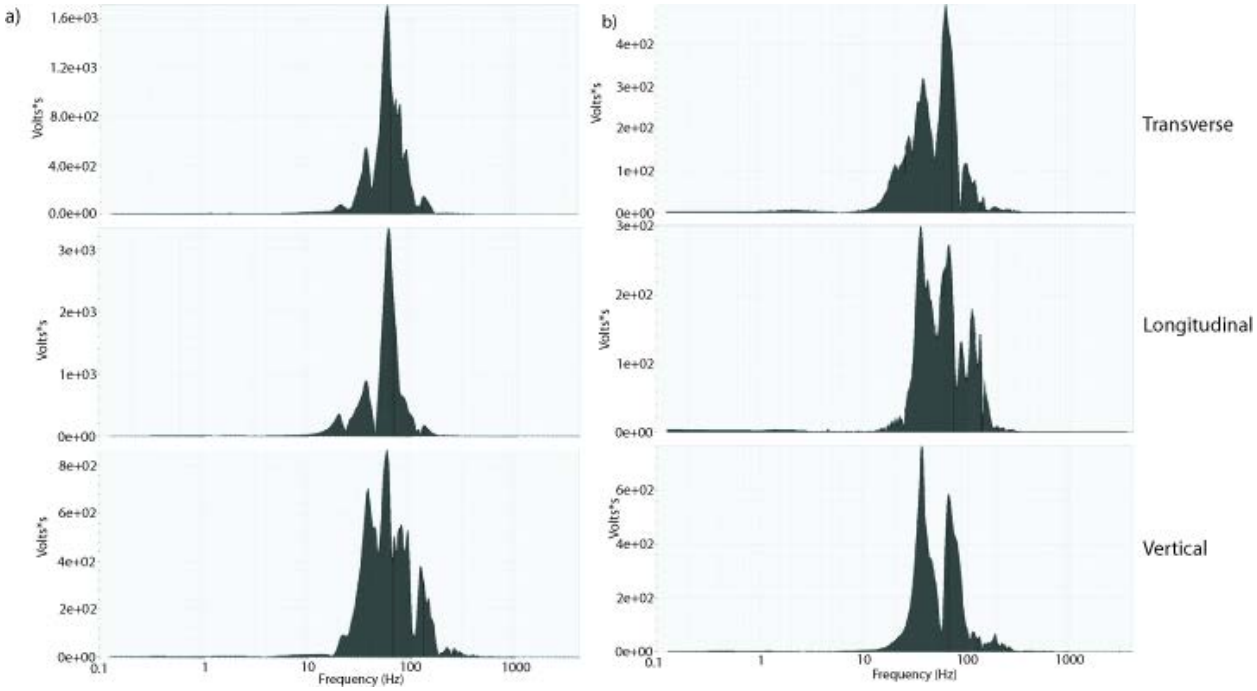


**Figure 8. Frequency spectrum for all three components of the a) 5 ft (1.5 m) red and b) 35 ft (10.7 m) blue surface geophones from a 2000 psi (13.8 MPa) shot located 30 ft (9.1 m) from the canal wall.**

## Experiment 2: In-line and Offset Geophone PPVs

### Ground Vibrations at Geophones In-line from a 2000 psi Shot

The configuration for this experiment was described in Chapter 2 (Figure 13). The differences between ground vibrations "in-line" (laterally offset only 5 ft [1.5 m] from the shot) and offset (15 ft or 4.6 m) were assessed for the surface geophones 5 ft (1.5 m) from the canal wall. In-line was the white geophone and offset was the red geophone. The water gun was located 40 ft (12.2 m) into the canal operating at a pressure of 2000 psi (13.8 MPa). Thus the angle in plan view between the shot is 5 degrees for the in-line geophone and 13.2 degrees for the offset geophone. Comparison PPV results between the in-line and offset geophones for a single 2000 psi (13.8 MPa) shot located 40 ft (12.2 m) from the canal wall are displayed in Table 4. PPV for the transverse and vertical components are similar between the in-line and offset shots. The longitudinal component, however, exhibits an almost 4-fold increase in PPV for the offset geophone, probably due to refracting at the canal wall. This will be discussed in the next chapter.

Table 4

In-line vs Offset Surface PPV Comparison

| | Transverse<br><br>in/s<br>(mm/s) | Longitudinal<br><br>in/s<br>(mm/s) | Vertical<br><br>in/s<br>(mm/s) | Sum Component Vector<br><br>in/s<br>(mm/s) |
|---|---|---|---|---|
| In-line | 0.053<br>(1.35) | 0.048<br>(1.22) | 0.070<br>(1.78) | 0.10<br>(2.54) |
| Offset | 0.111<br>(2.82) | 0.191<br>(4.85) | 0.113<br>(2.87) | 0.25<br>(6.35) |

Double Gun

The same in-line and offset configurations were used for the double-gun shots in Experiment 2. Guns were deployed 40 (12.2 m) and 120 ft (36.6 m) into the canal and simultaneously fired. The firing was not perfectly synchronized, however, leading to a somewhat complex wavelet, as shown in Figure 20. The corresponding PPVs of Figure 20 for a double gun shot are displayed in Table 5.

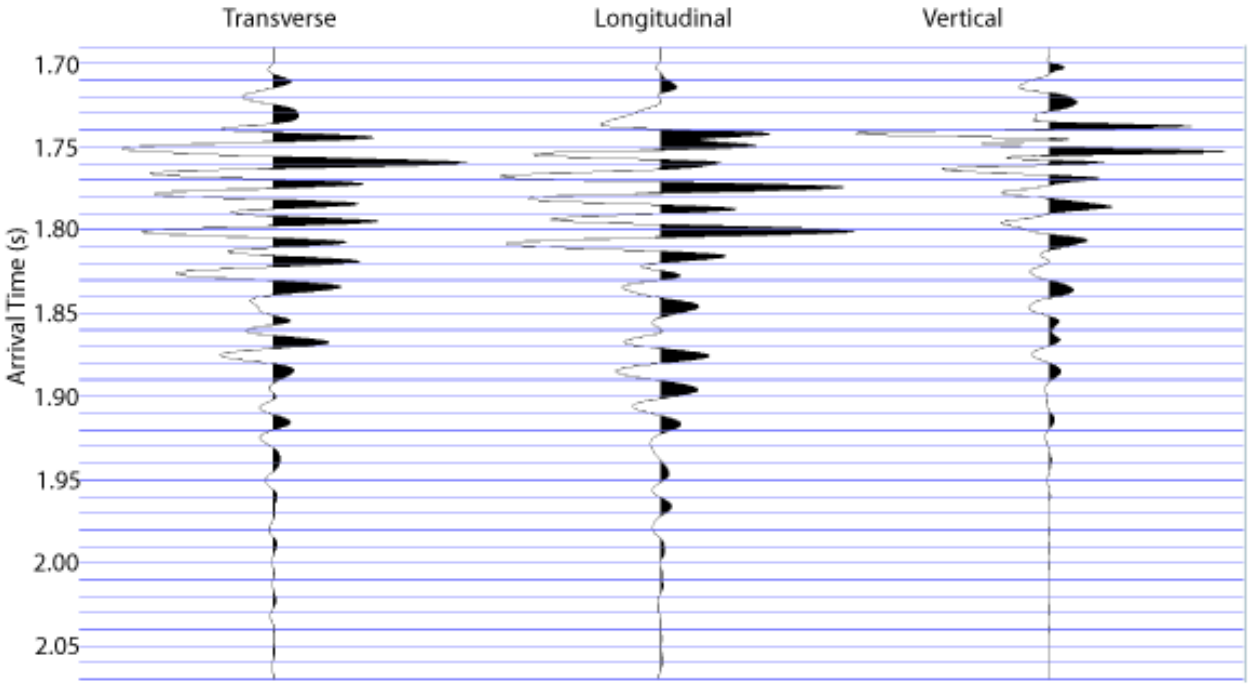


**Figure 20. Wavelets of all three components recorded at the 5 ft (1.5 m) from the canal white surface geophone from a double gun shot at 2000 psi (13.8 MPa) 40 ft (12.2 m) from the canal wall.**

Table 5

Comparison of In-line Geophone PPVs Produced by a Double Gun Shot and Single Gun Shot

| | Transverse<br><br>in/s<br>(mm/s) | Longitudinal<br><br>in/s<br>(mm/s) | Vertical<br><br>in/s<br>(mm/s) | Sum Component Vector<br><br>in/s<br>(mm/s) |
|---|---|---|---|---|
| Both Guns | 0.08<br>(2.03) | 0.05<br>(1.27) | 0.12<br>(3.05) | 0.15<br>(3.81) |
| North Gun | 0.08<br>(2.03) | 0.08<br>(2.03) | 0.12<br>(3.05) | 0.16<br>(4.06) |

## Experiment 3: Effect of Different Shot Pressures

### Comparing 1000 and 2000 psi (6.9 and 13.8 MPa) Shot Ground Vibrations at In-line Geophones

The configuration for this experiment was described in Chapter 2 (Figure 14). The differences between ground vibrations of 1000 and 2000 psi (6.9 and 13.8 MPa) shots in-line with a water gun shot 40 ft (12.2 m) from the canal wall are displayed in Table 6. Not surprisingly, the peak ground velocity decreases with the decrease in gun pressure for the transverse and vertical components. Interestingly, the longitudinal component velocity remains about the same.

Table 6

1000 vs 2000 psi PPV Comparison

| | Transverse<br><br>in/s<br>(mm/s) | Longitudinal<br><br>in/s<br>(mm/s) | Vertical<br><br>in/s<br>(mm/s) |
|---|---|---|---|
| 1000 psi | 0.054<br>(1.37) | 0.050<br>(1.27) | 0.069<br>(1.75) |
| 2000 psi | 0.080<br>(2.03) | 0.048<br>(1.22) | 0.123<br>(3.12) |

## Background Noise

Background noise sources within the CSSC include the natural background noise of the area, (roads, railroads, aircraft, industrial and construction activities), commercial, private boat traffic, and footsteps. The PPV for different background noise sources from both the 2011 and 2014 surveys are displayed in Table 7 (Carpenter et al., 2015).

Table 7

Background Noise (Vertical Component) Along the CSSC

| Source | Ground Vibration<br><br>in/s<br>(mm/s) |
|---|---|
| Natural Background | 1.47 E^-4<br>(3.73 E^-3) |
| Barge | 8.58 E^-5<br>(2.18 E^-3) |
| Leisure Boat | 8.44 E^-5<br>(2.14 E^-3) |
| Railway (near EFB) | 2.50 E^-4<br>(6.35 E^-3) |
| Power Plant | 2.80 E^-3<br>(7.11 E^-2) |

Some of the shots showed pre- and post-water gun exposure noise linked with someone walking by a surface geophone or hammering on the iron borehole casing 35 ft (10.7 m) from the canal. This noise was not present during the water gun shots – walking and all other activities were suspended during the shooting. The maximum ground vibrations of these sources depend on their locations in relation to the geophone. For example, footsteps on the transverse side of a geophone will produce a larger transverse ground vibration value than on the longitudinal side. Walking and hammer noise PPVs of all three components are shown in Table 8. In general background noise is, at most, 1/10 that of the PPV from the water gun. Thus the excitation of the canal walls by these various sources is not comparable to that produced by the water gun.

Table 8

Walking and Hammer Background Noise

| Source | Transverse<br>in/s<br>(mm/s) | Longitudinal<br>in/s<br>(mm/s) | Vertical<br>in/s<br>(mm/s) |
|---|---|---|---|
| Walking | 0.004<br>(0.102) | 0.006<br>(0.152) | 0.006<br>(0.152) |
| Hammer | 0.020<br>(0.508) | 0.013<br>(0.330) | 0.017<br>(0.432) |

# CHAPTER 4

# DISCUSSION

## Experiment 1: Ground Motion vs. Shot Distance

### Maximum Amplitude and Wavelet Repeatability

As noted in the previous chapter, the ground vibration wavelets resulting from single water gun discharge are remarkably repeatable, with the major peak of each wavelet occurring at the same time, relative to the start of the wavelet. The peak amplitude (or PPV) of these wavelets are also very repeatable. This suggests a consistent water gun pulse, with the water gun orientation and discharge pressure remaining constant; coupling of the pressure wave into the canal wall is also consistent from shot-to-shot.

## Change in Maximum Amplitude (PPV) with Increasing Shot Distance from the Canal Wall

### Vertical Component

The larger PPV values are recorded by the 5 ft (1.5 m) surface geophone: seismic wave energy significantly attenuates by the time it reaches the 35 ft (10.7 m) surface geophone. There is also greater variability between PPV values recorded at the 5 ft (1.5 m) geophone compared to the 35 ft (10.7 m) geophone. The vertical PPV for both the 5 (1.5 m) and 35 ft (10.7 m) geophones appear to decrease linearly as shot distance from the canal wall (the shore) increases. This linear decreasing trend is also seen in both the borehole geophones' vertical component. This relationship allows an estimation of the vertical ground vibration at a theoretical shot distance of zero (i.e. along the canal wall, which has been suggested as a water gun placement so as not to interfere with barge traffic). Thus, the maximum vertical ground vibration that the wall would experience along its edge at the surface would be 0.13 in/s (3.3 mm/s), from extrapolation of the Figure 21 least-squares lines to a shot distance of 0 ft (0 m). The $R^2$ value of 0.88 of the 5 ft (1.5 m) vertical interpolation line signifies good correlation.

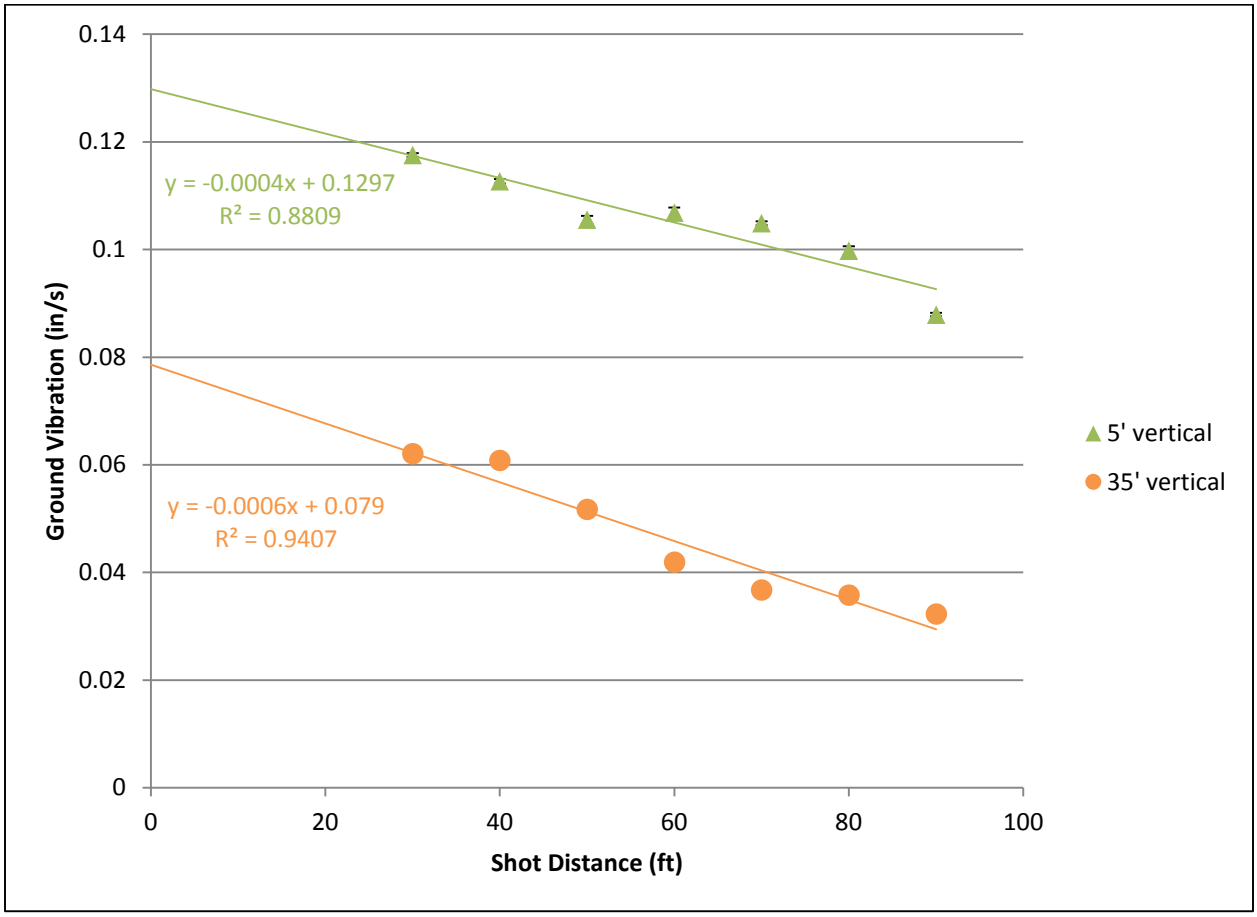


**Figure 21. Change in vertical component ground vibrations with extrapolation lines as shot distance increases for the 5 and 35 ft (1.5 and 10.7 m) surface geophones from a 2000 psi (13.8 MPa) shot.**

Horizontal Components

The PPV for the two horizontal components at the 35 ft (10.7 m) geophone also decrease linearly as shot distance from the canal wall increases. However, trends for the geophone 5 ft (1.5 m) from the

canal wall horizontal components appear to be more complex. The 5 ft (1.5 m) transverse component PPV exponentially decreases as shot distance increases. The 5 ft (1.5 m) longitudinal component could be considered linear; however it shows a kink in its linear decrease between shot distances of 60 and 70 ft (18.3 and 21.3 m) possibly signifying a P- to S-wave conversion at this distance, which will be explained later in this chapter. This component actually produces the highest PPV values but estimating the maximum ground vibrations at the 5 ft (1.5 m) geophone for a shot along the wall may not be exact because we do not know if there is another change in ray travel path (i.e. another "kink") between 0 and 30 ft (0 and 9.1 m) shot distances. If there is no kink, the estimated maximum ground movement is 0.30 in/s (7.62 mm/s) (Figure 22).

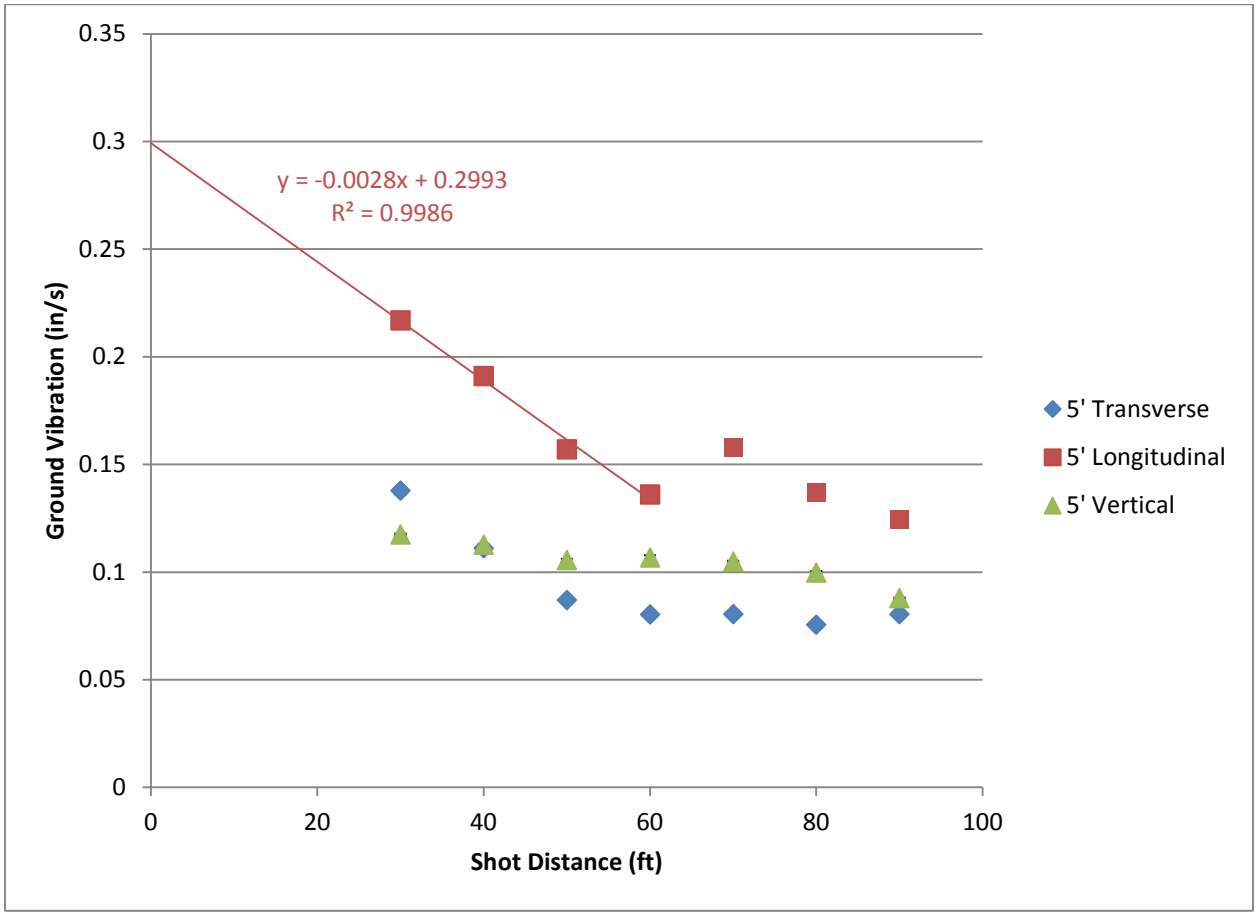


**Figure 22. Change in ground vibrations for the 5 ft (1.5 m) surface geophone from a 2000 psi (13.8 MPa) shot from gun #1. This graph also displays the extrapolation of the 5 ft (1.5 m) longitudinal component to estimate the ground vibrations produced from a shot distance of 0 ft (0 m) assuming there is no "kink" between the 0 and 30 ft (0 and 9.1 m) shot distances.**

## Practical Application

Ground vibrations from the water gun might only affect vibration-sensitive facilities located right next to the canal according to ground vibration damage criteria from Drogan (2013). The United States Bureau of Mines (USBM) established a practical safe threshold to ensure that no damage occur to buildings near blasting sites. This threshold is generally accepted at 0.75 in/s (19.1 mm/s) for “modern” buildings constructed with drywall and 0.50 in/s (12.7 mm/s) for “older” buildings constructed with plaster (Siskind et al., 1980). The recorded PPVs of the water gun are far below the level that would cause damage, which is generally accepted to be 0.75 in/s (19.05 mm/s). This implies that structures along the canal wall will most likely not be damaged by water gun shots.

## Sum Component Vector for Maximum Ground Motion

### Maximum PPV in 3-dimensions

The 5 ft (1.5 m) surface geophone records the maximum ground vibrations produced by the water gun. The mean sum component vector value for this location is 0.28 in/s (7.11 mm/s). This sum

component vector value is still well below the 0.75 in/s (19.05 mm/s) PPV damage threshold established by the USBM, which implies that there is no potential for damage to buildings located along the canal (Figure 23). The survey area ground vibration map indicates that ground movement decreases with increasing distance from the shot, and more movement (ground velocity) is recorded at the ground surface and at 25 ft (7.6 m) bgs, equivalent to the mid-level of the canal with the ground surface always experiencing higher values. A higher value is recorded at about 25 ft (7.6 m) bgs compared to 5 ft (1.5 m) bgs due to the depth of the water gun. The deeper borehole geophones were more directly in-line with the water guns and thus experienced a more direct blast from the shot.

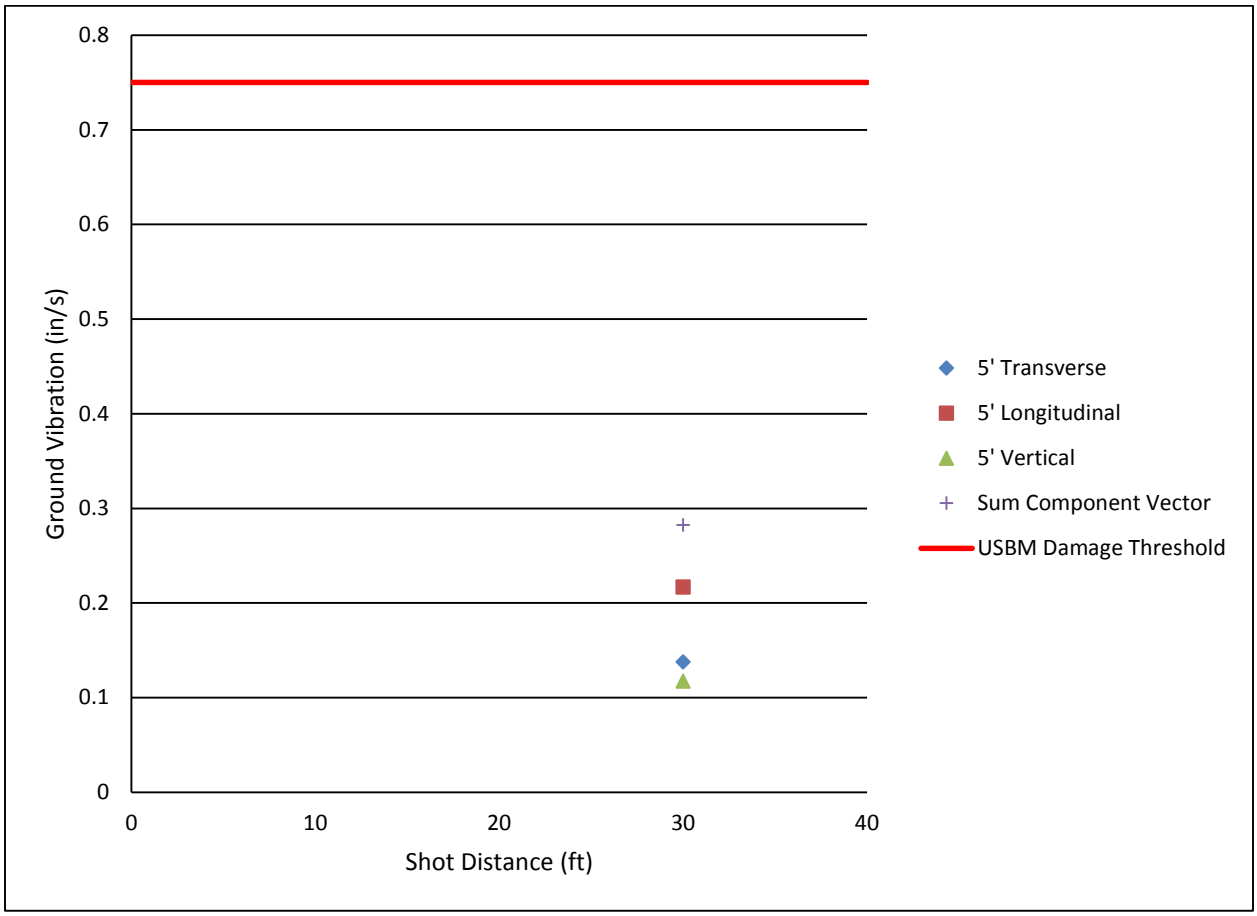


**Figure 23. Comparison of the PPV values recorded (transverse, longitudinal, vertical, and sum component vector) at the 5 ft (1.5 m) surface geophone from a 2000 psi (13.8 MPa) shot located 30 ft (9.1 m) from the canal wall with respect to the ground vibration damage threshold established by the USBM.**

## Fatigue Issues

It is still unknown how repeated exposure to the water gun over a prolonged period of time will affect structures built along the canal, structures built near the water gun, or even to the canal itself, and this should be monitored in the future. It may be difficult to determine if the water gun is the source of building cracks as all homes eventually crack because of a variety changes like temperature and humidity, consolidation, variation in ground moisture and wind (Siskind et al., 1980) so consistent monitoring will be key to analyze long-term exposure.

## Double Gun

Since the water guns were discharged manually, it was difficult to time them to go off simultaneously; we see this in the resulting wavelets and PPVs produced. PPVs for a double gun shot are roughly the same, even slightly smaller, than a single gun shot at the same distance possibly due to some interference between the seismic waves. Examining the wavelets produced by the double gun we see two major peaks in the vertical component, which implies that the guns were not set off simultaneously. This could possibly be fixed by using an automated system, as is used in the seismic exploration industry. Multiple saddles are found in both horizontal components signifying interference between the two gun shots. If an automated system were used to set off the water guns, there could be significant changes in the maximum ground vibrations felt by the canal wall.

## Frequency Content

For the geophone 5 ft (1.5 m) from the canal wall, the vertical component spectrum peaks at about 40 and 90 Hz and at about 60 and 80 Hz for the horizontal components. The geophone 35 ft (10.7 m) from the canal wall has frequency peaks at about 40, 56, and 84 Hz for all three components. The dominant frequency of ground motion produced by the water gun is primarily above 40 Hz. According to Drogan (1999) and the USBM, frequencies less than 40 Hz pose a higher threat than its higher frequency counterparts because the wave energy attenuates more slowly over time and distance, and thus has the potential to cause damage to objects further away from the source. The dominant frequencies produced by the water gun are above 40 Hz, so the wave energy should attenuate quickly with distance from the canal wall, with little disturbance to structures further from the wall.

## Experiment 2: In-line and Offset Geophones

### Ground Vibrations at Geophones In-line from a 2000 psi Shot

The vertical component is highest at the in-line geophone while the longitudinal is highest at the offset geophone. Since the maximum ground vibration recorded changes between components, it

suggests that the travel path of a water gun seismic wave changes with lateral offset. Figure 24 displays the potential ray paths for the water gun's seismic wave.

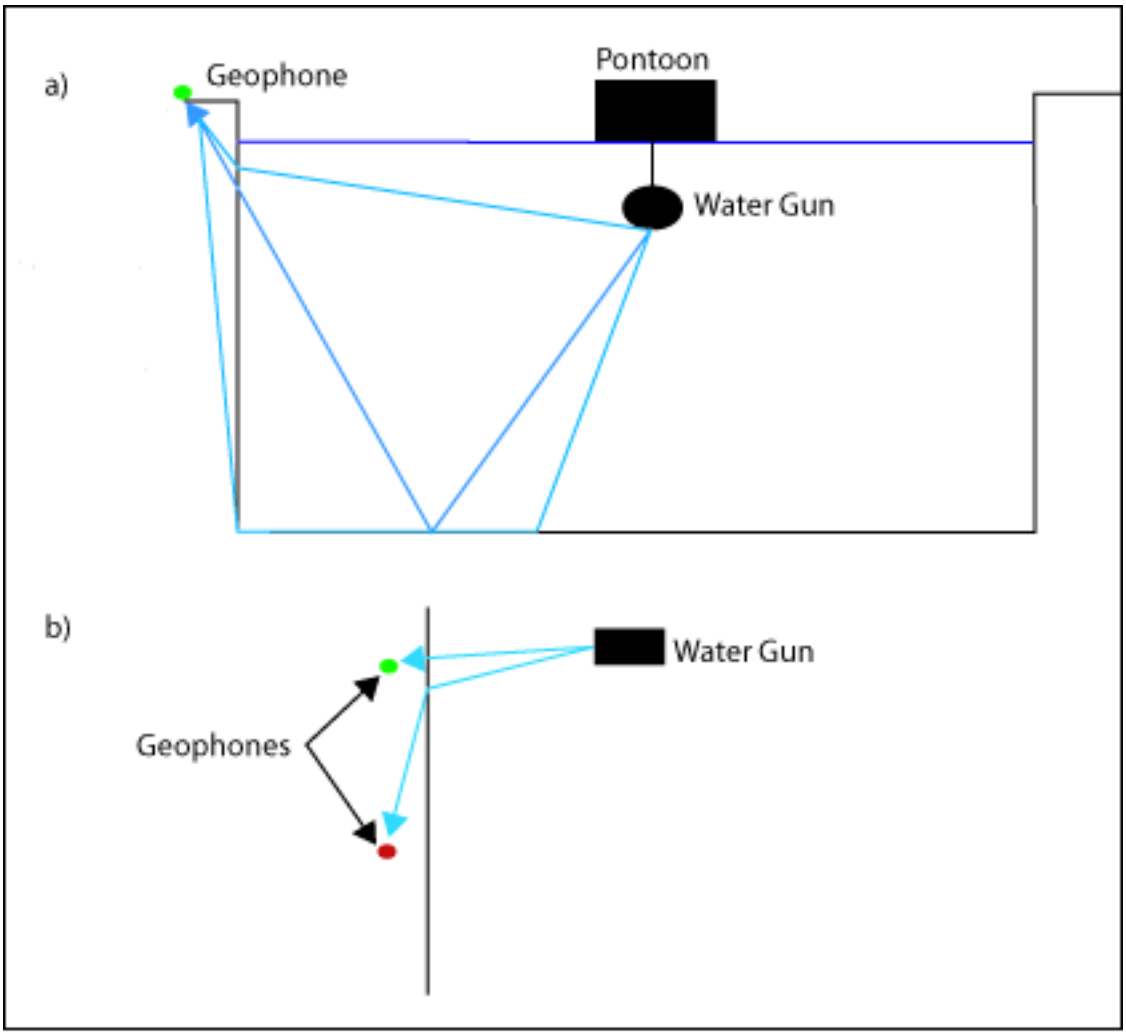


**Figure 24. a) A cross-sectional view of the water gun's seismic ray path for the in-line geophones showing that the in-line geophone is receiving seismic waves that are reflected or refracted off the canal bottom to cause greater movement in the vertical direction. b) A plane view of the water gun's seismic ray path for the offset geophones showing that the offset geophone is receiving seismic waves refracting at the canal wall instead of the canal bottom to cause greater movement in the longitudinal direction.**

Modeling the Response for Experiments 1 and 2

Some insights can be gained by looking quantitatively at the ray paths' incidence and emergence angles (Figure 25). Since the velocity of the dolomite and geometry of the survey are known, Fermat's Principle can be applied to calculate the incident and refraction angles of the water gun ray path. Fermat's Principle involves rays that take the minimum time path between two points (Sheriff and Geldart, 1995).

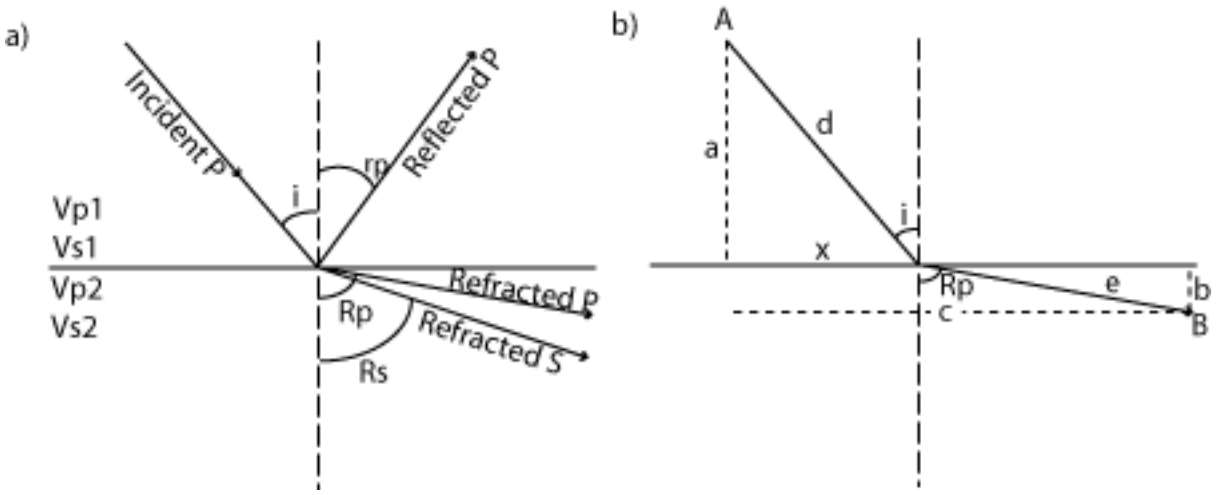


**Figure 25. a) Four generated waves that are produced when a P-wave strikes a velocity discontinuity and b) the resulting geometry to determine the minimum time between points A and B, Snell's Law may be used to calculate the incident angle (i) and refraction angle (Rp).**

From the geometry of the above diagram, for incident and refracted P waves,

$$\sin i = \frac{x}{d} = \frac{x}{\sqrt{a^2+x^2}}, \qquad (2)$$

and

$$\sin R_P = \frac{(c-x)}{\sqrt{(c-x)^2+b^2}} . \quad (3)$$

From Snell's Law $\frac{\sin i}{\sin R_P} = \frac{V_{P_1}}{V_{P_2}}$ , so $\sin Rp = \sin i \,(\frac{V_{P_2}}{V_{P_1}})$ , so,

$$\frac{V_{P_2}}{V_{P_1}} \sin i = \frac{(c-x)}{\sqrt{(c-x)^2+b^2}} . \quad (4)$$

Thus two simultaneous equations must be solved with two unknowns, x and i:

$$\sin i = \frac{x}{\sqrt{x^2+a^2}} \text{ , and} \quad (5)$$

$$\frac{V_{P_2}}{V_{P_1}} \sin i = \frac{(c-x)}{\sqrt{(c-x)^2+b^2}} . \quad (6)$$

Dividing equation (6) by equation (5),

$$\frac{V_{P_2}}{V_{P_1}} = \frac{(c-x)\sqrt{x^2+a^2}}{x\sqrt{(c-x)^2+b^2}} . \quad (7)$$

The horizontal components, transverse and longitudinal, may be primarily recording S-waves converted from P waves at the canal wall. Thus to accommodate S-waves the following expression must be used:

$$\frac{V_{S_2}}{V_{S_1}} = \frac{(c-x)\sqrt{x^2+a^2}}{x\sqrt{(c-x)^2+b^2}} . \quad (8)$$

Note that $V_{S_1}$ does not exist since only P-waves can travel through water. Solving for x algebraically can be arduous, so a numerical approach was used. $\frac{V_{P_2}}{V_{P_1}}$ was computed and various values of x were tried in the right side of the equation until both sides matched. Once x was obtained then i and Rp, Rs could be computed.

Experiment 1 Models

P-wave Refraction. For experiment 1, a = 30 ft (9.1 m), b = 5 ft (1.5 m), and c = 15 ft (4.6 m). Estimated velocities are Vp1 = 5000 ft/s (1500 m/s) and Vp2 = 20000 ft/s (6000 m/s). The geophone and shot locations using GPS data for experiment 1 are shown in Figure 26. The following values in Table 9 were obtained through modeling using the MATLAB routine incidence.m (shown in Appendix B). The no solution notation tells us that P-waves cannot propagate as first arrivals at these geometries. Thus, we need to look at P- to S-wave conversions at these angles. P- to S-wave conversions and S-wave refraction angles in the horizontal direction are shown in Table 10.

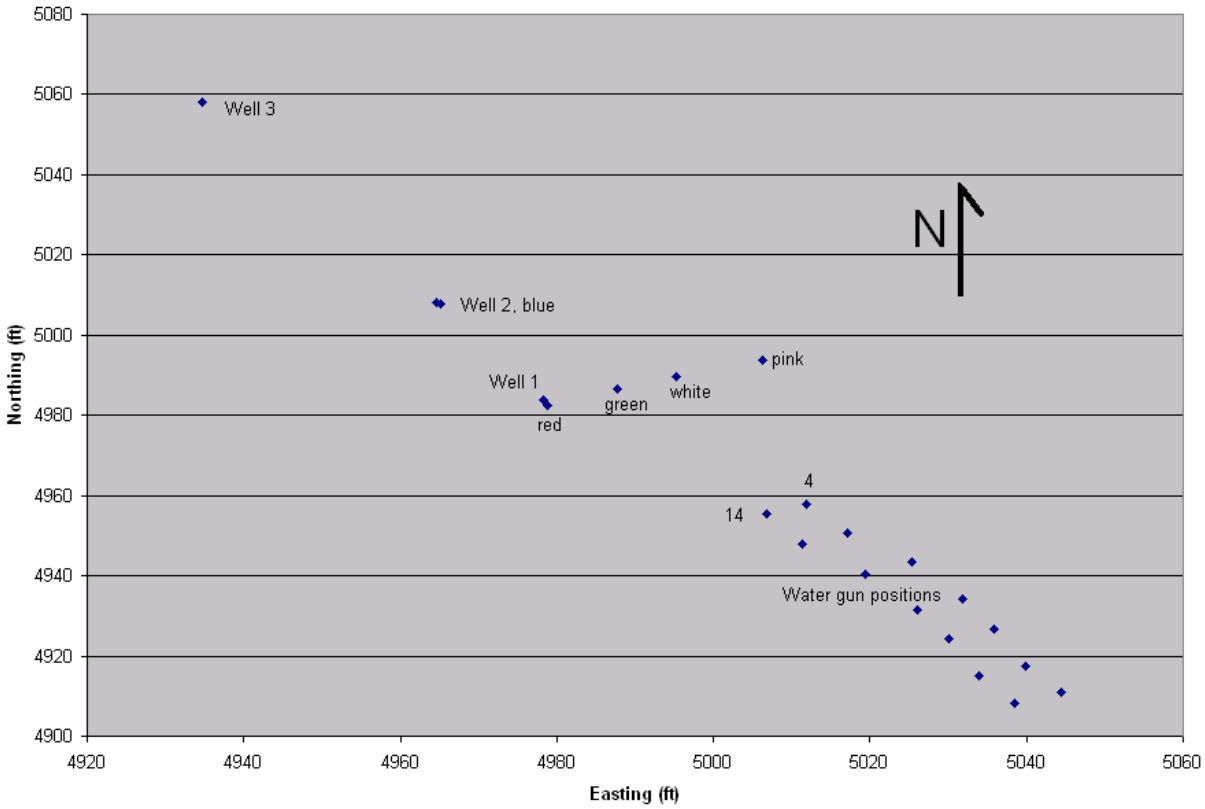


**Figure 26. Position of the geophones, wells, and water gun shots for Experiment 1 generated from GPS data.**

**Table 9**

**P-wave Incidence and Refraction angles as shot distance increases**

| Shot distance<br>ft<br>(m) | Incidence angle<br>(°) | Refraction angle<br>(°) |
|---|---|---|
| 30<br>(9.1) | 14.5 | 77.3 |
| 40<br>(12.2) | 14.4 | 75.8 |
| 50<br>(15.2) | 14.3 | 73.9 |
| 60<br>(18.3) | 14.0 | 71.6 |
| 70<br>(21.3) | No solution | No solution |
| 80<br>(24.4) | No solution | No solution |
| 90<br>(27.4) | No solution | No solution |

**Table 10**

**P- to S-wave Conversion Incidence and S-wave Refraction Angles as Shot Distance Increases**

| Shot distance<br>ft<br>(m) | Incidence angle<br>(°) | Refraction angle<br>(°) |
|---|---|---|
| 30<br>(9.1) | 27.2 | 71.1 |
| 40<br>(12.2) | 25.9 | 64.7 |
| 50<br>(15.2) | 24.0 | 57.2 |
| 60<br>(18.3) | 21.8 | 50.3 |
| 70<br>(21.3) | 19.7 | 44.4 |
| 80<br>(24.4) | 17.9 | 39.6 |
| 90<br>(27.4) | 16.4 | 35.7 |

The refraction angle favors the longitudinal S-wave at values greater than about 45°, starting at a distance of approximately 70 ft (21.3 m) from shore. This is also where the “kink” is seen on the

longitudinal component vs. shot distance graph (Figure 17). S-waves are more complicated than P-waves because they contain both SV and SH components, so vibration can be either along the propagation direction or perpendicular to it (P.J. Carpenter, personal communication, June 22, 2015). Thus with even large angle of refraction, the longitudinal component may dominate.

Experiment 2 Models:

Geophone Lateral Offset = 5 ft (1.5 m). For Experiment 2, a = 40 ft (12.2 m), b = 5 ft (1.5 m) and c = 5 ft (1.5 m). Estimated velocities are Vp1 = 5000 ft/s (1500 m/s) and Vp2 = 20000 ft/s (6100 m/s). The following calculation assumes a horizontal travel path. Solving equation (7) using MATLAB (program incidence.m, included in Appendix B), gives a solution of x = 3.4 ft (1.04 m), i = 4.86°, and Rp = 17.7°.

A P- to S- wave conversion at the canal wall produces the following values: x = 4.0 ft (1.22 m), i = 5.64° and Rs = 11.9°.

For the vertical section, a = 40 ft (12.2 m), b = 5 ft (1.5 m), and c = 20 ft (6.1 m), and the shot is submerged 14 ft (4.3 m). The line is assumed to be perpendicular to the shore. This produces an x = 10.2 ft (3.1 m), i = 14.3° and an Rp = 63°, suggesting the vertical component should be largest, which is observed.

Geophone Lateral Offset=15 ft (4.6 m). In this case, a = 40 ft (12.2 m), b = 5 ft (1.5 m) and c = 15 ft (4.6 m). Estimated velocities are the same. Here the solution is x = 8.8 ft (2.7 m), i = 12.5° and Rp = 51°, suggesting both the transverse and longitudinal components should be about the same as the P-wave. For the P- to S-wave conversion at the canal wall, x = 11.5 ft (3.5 m), i = 16.1° and Rs = 34.9°,

suggesting the longitudinal component should be the largest, which is observed (Table 4). The case of the 15 ft (4.6 m) lateral offset could not be modeled as a vertical section due to the substantial horizontal motion—this case is a 3-dimensional (3D) problem (P.J. Carpenter, personal communications, June 8, 2015).

## Double Gun

As stated in the double gun shots of experiment 1, the water guns were triggered manually so firing simultaneously could not be achieved consistently. Again, the wavelets are more complicated compared to the single water gun shot. In the wavelet of the double gun shot, we see two separate distinct peaks in the vertical component. These peaks are due to the separation between the water guns and/or delays in firing. The ground vibrations produced by the 40 ft (12.2 m) water gun will hit the canal wall before those produced by the 120 ft (36.6 m) water gun, thus the first peak in the wavelet corresponds to the 40 ft (12.2 m) water gun while the second peak corresponds to the 120 ft (36.6 m) water gun (refer back to Figure 20). It will not matter if the guns go off simultaneously or not at this gun orientation because the ground vibrations of the 40 ft (12.2 m) gun will always reach the canal wall first and there will be no constructive interference between the two guns.

## Experiment 3: Effects of Different Shot Pressures

### Comparing 1000 and 2000 psi (6.9 and 13.8 MPa) Shot Ground Vibrations at In-line Geophones

A difference in shot pressure doesn't change which component records the highest PPV value, it only affects the maximum amplitude of the ground vibrations as shown in Table 6. For an in-line shot, the vertical component always records the highest value. Decreasing the shot pressure by half does not also halve the PPV; in fact, the transverse and vertical components declined by more than 50%. The longitudinal component remains more or less the same as shot pressure changes.

### Background Noise

Background, barge and leisure boat noise values were very small, on the order of 10^-3 to 10^-5 in/s (10^-2 to 10^-4 mm/s), while walking and hammering noise values were much higher, with PPVs in the range of 0.02 in/s (0.51 mm/s). The PPV of background noise is much lower than the PPV of the water gun and thus should not impact the PPVs experienced by the canal wall. Overall, the impact of background noise is negligible.

# CHAPTER 5

# CONCLUSION

The ground vibrations produced by an 80 $in^3$ (1.31 L) water gun on the Chicago Sanitary and Ship Canal in Lemont, Illinois were recorded and analyzed to determine if they threaten damage to the CSSC and to structures along the canal. In the first configuration, the change in ground vibrations was recorded as a function of gun distance from the shore. The second configuration compared the ground vibrations in-line with those offset from the shot. Finally, the third configuration revealed how a change in shot pressure affected the ground vibrations experienced by the canal wall.

The first configuration (experiment 1) revealed that ground vibrations produced by a single 2000 psi (13.8 MPa) water gun shot 30 ft (9.1 m) from the canal wall are much lower than the damage threshold established by the USBM. Even the sum component vector was well below this limit so, in theory, if two water guns were deployed and fired simultaneously, their resulting ground vibrations (i.e. PPV) potentially could double and still be below the damage threshold. Using the trends established, even at a shot distance of 0 ft (0 m) the ground vibrations are still below the threshold, meaning the water guns could safely be deployed along the canal walls. The second configuration proved that the water gun's seismic ray path changed with receiver position along the canal wall relative to the water; this is seen by the change in which component recorded the highest ground vibrations between the in-line and offset

geophones. Higher PPVs were also recorded for the longitudinal component at larger offsets from a water gun shot. Also, the calculation of incident and refraction angles between the in-line and offset geophones indicate the point on the canal wall where the ray refracts changes as the geophone moves away from the source. Lastly, in the third configuration, doubling of the water gun firing pressure does not double the ground vibrations produced. The water gun firing pressure could be much higher and still produce ground vibrations below the USBM threshold. USACE has established a canal wall water pressure (i.e. the pressure in the water, not gun firing pressure) threshold of 5 psi (0.03 MPa), so the ground vibrations produced will be constrained to a considerably degree by the water pressure.

It is highly recommended that a series of future studies be carried out to better understand water gun exposure on the CSSC. Long term monitoring could determine if prolonged exposure would result in damage to the canal itself or to structures along the canal. In particular, fatigue issues predominate, given that the water guns would be firing about every 5-10 seconds for several years. It could also reveal whether the Asian carp response decreases over time as literature might suggest. Larger water gun arrays should be tested because additional water guns may be needed at places where the canal is wider. Also, logical placement of the water guns, e.g. along the canal wall and bottom, should be considered so that they will not interfere with the daily functions of the canal.

REFERENCES


Alonzo, B. (2013). *Evaluating ground motion produced by a seismic water gun used to control invasive Asian carp*. (Unpublished senior honors thesis). Northern Illinois University, IL.

Boeger, W.A., Pie, M.R., Ostrensky, A., and Cardoso, M.F. (2006). *The effects of exposure to seismic prospecting on coral reef fishes*. Brazilian Journal of Oceanography, 54 (4), 235-239.

Bretz, H.J. (1955). *Geology of the Chicago Region Part II—The Pleistocene*. Illinois State Geological Survey, Bulletin 65.

Britton, J.R., Gozlan, R.E., and Copp, G.H. (2011) *Managing non-native fish in the environment*. Fish and Fisheries, 12 (3), 256-274, doi: 10.1111/j.1467-2979.2010.00390.x.

Carpenter, P.J., Morrow, W.S., Koebel, C.M., and Adams, R.F. (2015, May). *Comparison of ground motion from industry and barge traffic at the Chicago Sanitary and Ship Canal to vibrations from the Asian carp water gun.* 47 (5), 67. Poster presented at the GSA North-Central Section Meeting, Madison, WI.

Chapman, D.C. and Hoff, M.H. (2006). *Invasive Asian carps in North America*. American Fisheries Society Symposium, 74, 1-3.

Cudmore, B. and Mandrak, N.E. (2011). *Assessing the biological risk of Asian carps to Canada*. American Fisheries Society Symposium, 74, 15-30.

Dowding, C.H. (1985). *Blast vibration monitoring and control*. Englewood Cliffs, NJ: Prentice-Hall.

Geometrics Seismodule Controller (Version 11.1.69.0) [Software]. Available from http://www.geometrics.com/geometrics-products/seismographs/download-seismograph-software/

Geopsy. (Version 2.7.0) [Software]. Available from http://www.geopsy.org/download/php

Global Earthquake Explorer (Version 2.2.0) [Software]. Available from http://www.seis.sc.edu/gee/download.html

Gordon, J.C.D., Gillespie, D., Potter, J., Frantzis, A., Simmonds, M.P., Swift, R., and Thompson, D. (2004). *A Review of the effects of seismic survey on marine mammals.* Marine Technology Society Journal, 37 (4), 16-34.

Heigold, P. (1990). *Seismic reflection and seismic refraction surveys in northeastern Illinois*. Illinois State Geological Survey Environmental Geology 136.

Hirst, A.G. and Rodhouse, P.G. (2000). *Impacts of geophysical seismic surveying on fishing success*. Reviews in Fish Biology and Fisheries, 10, 113-118.

Hutchinson, D.R. (1984). *Signature tests on 400-in³ water gun and 540-in³ air gun.* United States Department of the Interior Geological Survey. (Open-File Report 84-375).

Hutchinson, D.R. and Detrick, R.S. (1984). *Water gun vs air gun: A comparison*. Marine Geophysical Researches, 6 (3), 295-310.

Kelly, A.M., Engle, C.R., Armstrong, M.L., Freeze, M., and Mitchell, A.J. (2011). *History of introductions and government involvement in promoting the use of grass, silver, and bighead carps*. American Fisheries Society Symposium, 74, 163-174.

Koel, T.M., Irons, K.S., and Ratcliff, E. (2000). *Asian carp invasion of the upper Mississippi River system*. (US Geological Survey PSR 2000-05).

Kolar, C.S., Chapman, D.C., Courtenay Jr., W.R., Housel, C.M., Williams, J.D., and Jennings, D.P. (2007). *Bigheaded carps: a biological synopsis and environmental risk assessment*. American Fisheries Society, 33.

Leetaru, H.E., Sargent, M.L., and Kolata, D.R. (2004). *Geologic atlas of Cook County for planning purposes*. Illinois State Geological Survey.

Lillie, R.J. (1999). *Whole earth geophysics: An introductory textbook for geologists and geophysicists*. Upper Saddle River, NJ: Prentice-Hall.

Mandrak, N.E. and Cudmore, B. (2004). *Risk assessment for Asian carps in Canada*. Fisheries and Oceans Canada (Research Document 2004/103).

Morrow, W., Carpenter, P.J., Adams, R., and Yeskis, D.J. (2015). *Seismic data collection from water guns and industrial background sources in the Chicago Sanitary Ship Canal area*. US Geological Survey (in review).

Moy, P.B., Polls, I., and Dettmers, J.M. (2011). *The Chicago Sanitary and Ship Canal aquatic nuisance species dispersal barrier*. American Fisheries Society Symposium, 74,121.

Nico, L.G., Williams, J.D., and Jelks, H.L. (2005). *Black carp: biological synopsis and risk assessment of an introduced fish*. American Fisheries Society, 32.

Sheriff, R.E. and Geldart, L.P. (1995). *Exploration seismology.* Cambridge: Cambridge University Press.

Siskind, D.E., Stagg, M.S., Kopp, J.W., and Dowding, C.H. (1980). *Structure response and damage produced by ground vibration from surface mine blasting*. United State Department of Interior, United States Bureau of Mines (Report of Investigations 8507).

Sparks, R.E., Barkley, T.L., Creque, S.M., Dettmers, J.M., and Stainbrook, K.M. (2010). *Evaluation of an electric fish dispersal barrier in the Chicago Sanitary and Ship Canal*. American Fisheries Society Symposium, 74, 139-161.

Thomas, R.G., Jenkins, J.A., and David, J. (2011). *Occurrence and distribution of Asian carps in Louisiana*. American Fisheries Society Symposium, 74, 239.

Zeizel, A.J., Walton, W.C., Sasman, R.T., and Prickett, T.A. (1962) *Ground-water resources of DuPage County, Illinois*. Illinois State Geological Survey (Ground-water Report 2).

# APPENDIX A

# LEMONT EXPERIMENT DATA FILES

Two types of three-component (3C) sensors were deployed: R.T. Clark® 10 Hz surface geophones and R.T. Clark® 10 Hz downhole geophones. Each of the three components corresponds to channels as shown below:

R.T. Clark® 10 Hz surface geophones
Channel 1: transverse component
Channel 2: longitudinal component
Channel 3: vertical component

R.T. Clark® 10 Hz borehole geophones
Channel 1: transverse component
Channel 2: longitudinal component
Channel 3: vertical component

Orientation of transverse and longitudinal components within the borehole was unknown, due to rotation of the geophones before they were attached to the borehole wall. The relative orientation of components was established through tap tests.

## Experiment 1
## June 3, 2014

**Files 1.dat through 119.dat**

| **Channels** | **Sensor Location** |
|---|---|
| 1-3 | 5' borehole, shallow 3C geophone |
| 4-6 | 5' borehole, deep 3C geophone |
| 7-9 | 35' borehole, shallow 3C geophone |
| 10-12 | 35' borehole, deep 3C geophone |
| 13-15 | 100' borehole, shallow 3C geophone |
| 16-18 | 100' borehole, deep 3C geophone |
| 19-21 | 5' borehole, surface 3C geophone |
| 22-24 | 35' borehole, surface 3C geophone |

**Gun = 80 in³**

| **File** | **Shot size (psi)** | **Gun #** | **Gun distance from canal wall (ft)** |
|---|---|---|---|
| 1.dat-6.dat | troubleshooting | | |
| 7.dat-8.dat | barge | | |
| 9.dat-14.dat | 2000 | 1 | 90 |
| 15.dat-19.dat | 2000 | 2 | 90 |
| 20.dat-24.dat | 2000 | both | 90 |
| **File** | **Shot size (psi)** | **Gun #** | **Gun distance from canal wall (ft)** |
| 25.dat-29.dat | 2000 | 1 | 80 |
| 30.dat-34.dat | 2000 | 2 | 80 |
| 35.dat-39.dat | 2000 | both | 80 |
| 40.dat | barge | | |
| 41.dat-45.dat | 2000 | 1 | 70 |
| 46.dat-50.dat | 2000 | 2 | 70 |
| 51.dat-55.dat | 2000 | both | 70 |
| 56.dat-61.dat | 2000 | 1 | 60 |
| 62.dat-66.dat | 2000 | 2 | 60 |
| 67.dat-71.dat | 2000 | both | 60 |

| | | | |
|---|---|---|---|
| 72.dat | background noise | | |
| 73.dat-77.dat | 2000 | 1 | 50 |
| 78.dat-82.dat | 2000 | 2 | 50 |
| 83.dat-88.dat | 2000 | both | 50 |
| 89.dat-93.dat | 2000 | 1 | 40 |
| 94.dat-95.dat | 2000 | 2 | 40 |
| 96.dat | barge | | |
| 97.dat-99.dat | 2000 | 2 | 40 |
| 100.dat-104.dat | 2000 | both | 40 |
| 105.dat-109.dat | 2000 | 1 | 30 |
| 110.dat-114.dat | 2000 | 2 | 30 |
| 115.dat-119.dat | 2000 | both | 30 |

## Experiment 2
## June 4, 2015

**Files 120.dat through 287.dat**

(new sensor configuration)

| **Channels** | **Sensor Location** |
|---|---|
| 1-3 | 5’ borehole, shallow 3C geophone |
| 4-6 | 5’borehole, deep 3C geophone |
| 7-9 | 35‘ borehole, shallow 3C geophone |
| 10-12 | 35‘ borehole, deep 3C geophone |
| 13-15 | Pink surface 3C geophone 5‘ from canal wall and 15‘ upstream from shot |
| 16-18 | White surface 3C geophone 5‘ from canal wall and 5‘ upstream from shot |
| 19-21 | Green surface 3C geophone 5‘ from canal wall and 5‘ downstream from shot |
| 22-24 | Red surface 3C geophone 5‘ from canal wall and 15‘ downstream from shot |

**Gun = 80 in³**

| **File** | **Shot size (psi)** | **Gun #** | **Gun Distance from canal wall (ft)** |
|---|---|---|---|
| 120.dat | barge | | |
| 121.dat | background noise | | |
| 122.dat-126.dat | 2000 | 1 | 40 |
| **File** | **Shot size (psi)** | **Gun #** | **Gun Distance from canal wall (ft)** |
| 127.dat-131.dat | 2000 | both | 40/120 |
| 132.dat-136.dat | 2000 | 1 | 40 |
| 137.dat-141.dat | 2000 | both | 40/120 |
| 142.dat-146.dat | 2000 | 1 | 40 |
| 147.dat-151.dat | 2000 | both | 40/120 |
| 152.dat-156.dat | 2000 | 1 | 40 |
| 157.dat-161.dat | 2000 | both | 40/120 |
| 162.dat | 2000 | 1 | 40 |
| 163.dat | background noise | | |
| 164.dat-168.dat | 2000 | 1 | 40 |
| 169.dat-173.dat | 2000 | both | 40/120 |
| 174.dat-178.dat | 2000 | 1 | 40 |
| 179.dat-184.dat | 2000 | both | 40/120 |
| 185.dat-189.dat | 2000 | 1 | 40 |
| 190.dat-194.dat | 2000 | both | 40/120 |
| 195.dat-199.dat | 2000 | 1 | 40 |

| | | | |
|---|---|---|---|
| 200.dat-204.dat | 2000 | both | 40/120 |
| 205.dat-209.dat | 2000 | 1 | 40 |
| 210.dat-213.dat | 2000 | both | 40/120 |
| 214.dat | background noise | | |
| 215.dat-220.dat | 2000 | 1 | 40 |
| 221.dat-225.dat | 2000 | both | 40/120 |
| 226.dat-230.dat | 2000 | 1 | 40 |
| 231.dat-235.dat | 2000 | both | 40/120 |
| 236.dat-240.dat | 2000 | 1 | 40 |
| 241.dat-245.dat | 2000 | both | 40/120 |
| 246.dat-250.dat | 2000 | 1 | 40 |
| 251.dat-255.dat | 2000 | both | 40/120 |
| 256.dat-261.dat | 2000 | 1 | 40 |
| 262.dat-267.dat | 2000 | both | 40/120 |
| 168.dat-272.dat | 2000 | 1 | 40 |
| 273.dat-277.dat | 2000 | both | 40/120 |
| 278.dat-282.dat | 2000 | 1 | 40 |
| 283.dat-287.dat | 2000 | both | 40/120 |

## Experiment 3
## June 5, 2015

**Files 288.dat through 433.dat**

(new sensor configuration)

| **Channels** | **Sensor Location** |
|---|---|
| 1-3 | White surface 3C geophone, 5’ from canal wall and 5’ upstream from shot |
| 4-6 | Green surface 3C geophone, 5’ from canal wall and 5’ downstream from shot |
| 7-9 | Red surface 3C geophone, 5’ from canal wall and 15’ downstream from shot |
| 10-12 | Blue surface 3C geophone, 15’ from canal wall and 5’ upstream from shot |
| 13-15 | Pink surface 3C geophone, 15’ from canal wall and 5’ downstream from shot |
| 16-18 | - |
| 19-21 | 5‘ borehole, shallow 3C geophone |
| 22-24 | 5‘ borehole, deep 3C geophone |

**Gun = 80 in³**

| **File** | **Shot size (psi)** | **Gun #** | **Gun distance from canal wall (ft)** |
|---|---|---|---|
| 288.dat | background noise | | |
| 289.dat-292.dat | 1000 | 1 | 40 |
| 293.dat-297.dat | 1000 | both | 40/120 |
| 298.dat-302.dat | 1000 | 1 | 40 |
| 303.dat-304.dat | barge | | |
| 305.dat-309.dat | 1000 | both | 40/120 |
| 310.dat-314.dat | 1000 | 1 | 40 |
| 315.dat-319.dat | 1000 | both | 40/120 |
| 320.dat-324.dat | 1000 | 1 | 40 |
| 325.dat-329.dat | 1000 | both | 40/120 |
| 330.dat-334.dat | 1000 | 1 | 40 |
| 335.dat-339.dat | 1000 | both | 40/120 |
| 340.dat-344.dat | 1000 | 1 | 40 |
| 345.dat-349.dat | 1000 | both | 40/120 |
| 350.dat-354.dat | 1000 | 1 | 40 |

| | | | |
|---|---|---|---|
| 355.dat-359.dat | 1000 | both | 40/120 |
| 360.dat-364.dat | 1000 | 1 | 40 |
| 365.dat-369.dat | 1000 | both | 40/120 |
| 370.dat-374.dat | 1000 | 1 | 40 |
| 375.dat-379.dat | 1000 | both | 40/120 |
| 380.dat | background noise | | |
| 381.dat | leisure boat | | |
| 382.dat-386.dat | 1000 | 1 | 40 |
| 387.dat-391.dat | 1000 | both | 40/120 |
| 392.dat-396.dat | 1000 | 1 | 40 |
| 397.dat-401.dat | 1000 | both | 40/120 |
| 402.dat-407.dat | 1000 | 1 | 40 |
| 408.dat-412.dat | 1000 | both | 40/120 |
| 413.dat-417.dat | 1000 | 1 | 40 |
| 418.dat-422.dat | 1000 | both | 40/120 |
| 423.dat-427.dat | 1000 | 1 | 40 |
| 428.dat-431.dat | 1000 | both | 40/120 |
| 432.dat | background noise | | |
| 433.dat | 1000 | both | 40/120 |

# APPENDIX B

## PROGRAM INCIDENCE.M

Incidence P Horizontal.m

```
a=90.0; b = 5; c = 30;
v1=5000
v2=20000
ratio = v2/v1
for x = 0.1:0.01:15
   testratio = (c-x)*sqrt(x^2+a^2)/(x*sqrt((c-x)^2+b^2));
   if abs(ratio-testratio)< 0.1
   a
   x
   i = asin (x/sqrt(a^2+x^2))*57.3
   Rp = asin ((c-x)/sqrt((c-x)^2+b^2))*57.3
   else
   end
end
```

Incidence P Vertical.m

```
a=90.0; b = 5; c = 20;
v1=5000;
v2=18000
ratio = v2/v1
for x = 0.1:0.01:20
   testratio = (c-x)*sqrt(x^2+a^2)/(x*sqrt((c-x)^2+b^2));
   if abs(ratio-testratio)< 0.1
   x
   i = asin (x/sqrt(a^2+x^2))*57.3
   Rp = asin ((c-x)/sqrt((c-x)^2+b^2))*57.3
   else
   end
end
```

Incidence S.m

```
a=40.0; b = 5; c = 15;
v1=5000;
v2=10393;
diary on
ratio = v2/v1
for x = 0.1:0.01:15
   testratio = (c-x)*sqrt(x^2+a^2)/(x*sqrt((c-x)^2+b^2))
   x
   i = asin (x/sqrt(a^2+x^2))*57.3
   Rs = asin ((c-x)/sqrt((c-x)^2+b^2))*57.3
end
  diary off
```

Incidence S Horizontal.m

```
a=90.0; b = 5; c = 30;
v1=5000;
v2=10393
ratio = v2/v1
for x = 0.1:0.01:30
   testratio = (c-x)*sqrt(x^2+a^2)/(x*sqrt((c-x)^2+b^2));
   if abs(ratio-testratio)< 0.01
   x
```

```
    i = asin (x/sqrt(a^2+x^2))*57.3
    Rs= asin ((c-x)/sqrt((c-x)^2+b^2))*57.3
    else
    end
end
```

Incidence S Vertical.m

```
a=90.0; b = 5; c = 20;
v1=5000;
v2=10393
ratio = v2/v1
for x = 0.1:0.01:30
    testratio = (c-x)*sqrt(x^2+a^2)/(x*sqrt((c-x)^2+b^2));
    if abs(ratio-testratio)< 0.01
    x
    i = asin (x/sqrt(a^2+x^2))*57.3
    Rs= asin ((c-x)/sqrt((c-x)^2+b^2))*57.3
    else
    end
end
```

Incidence S Vertical 1.m

```
a=30.0; b = 5; c = 30;
v1=5000;
v2=10393
ratio = v2/v1
for x = 0.1:0.01:30
    testratio = (c-x)*sqrt(x^2+a^2)/(x*sqrt((c-x)^2+b^2));
    if abs(ratio-testratio)< 0.01
    x
    i = asin (x/sqrt(a^2+x^2))*57.3
    Rs= asin ((c-x)/sqrt((c-x)^2+b^2))*57.3
    else
    end
end
```